OPTIMIZATION OF COMPOSITE PARTS PLACEMENT IN AUTOCLAVE

OTOKLAV İÇERİSİNDE KOMPOZİT PARÇA YERLEŞİMİ OPTİMİZASYONU

GÖZDENUR KIRDAR

ASST. PROF. DR. DİCLEHAN TEZCANER ÖZTÜRK
Supervisor

PROF. DR. MURAT CANER TESTİK
Co- Supervisor

Submitted to

Graduate School of Science and Engineering of Hacettepe University

as a Partial Fulfillment to the Requirements

for the Award of the Degree of Master of Science

in Industrial Engineering

2020

DEDICATED

TO

My Mother and My Sister, Meral and Gizem

For supporting and encouraging me to believe in myself and

making me the person I am today

My Grandparents, Müzeyyen and Mustafa

For being my first teacher

My Husband, Volkan

For his unfaltering support, patience, faith and making it possible to complete this work with his love and support

My Dog, Pixel

For supporting me in her own way through this process

ABSTRACT

OPTIMIZATION OF COMPOSITE PARTS PLACEMENT IN AUTOCLAVE

Gözdenur KIRDAR

Master Thesis, Department of Industrial Engineering

Supervisor: Asst. Prof. Dr. Diclehan TEZCANER ÖZTÜRK

Co- Supervisor: Prof. Dr. Murat Caner TESTİK

August 2020, 69 Pages

In the production of composite parts, usually multiple parts are loaded into the autoclave in one batch. A typical autoclave curing cycle has three main phases and proceeds as follows: all parts are heated until they reach the curing temperature during the heat-up phase, they are then held at this temperature for a certain period of time during the dwell period, and then they are cooled in the cooling phase. The main goal in a curing cycle is the complete curing of all parts. In an ideal curing cycle, all parts reach the curing temperature at the same time, avoiding any over-curing. However, due to some factors such as part positions, geometries, total mass in the load, it is often not possible to realize this requirement without any delays between parts. The parts that reach the curing temperature earlier than the others are over-cured as much as it takes for the last part (the lagging part) to reach the curing temperature. This time delay can be monitored via thermocouples on all parts during the curing cycle and it affects the product quality to a great extent. If these delays are minimized, higher quality products can be produced. Another consideration is minimization of the total process duration by shortening the heat-up phase. This way, time and energy savings can be obtained.

In this work, we develop a two-stage approach to minimize both the time delay between parts and the duration of the heat-up phase. In the first stage, we determine the factors

affecting the time to reach the curing temperature. We divide the autoclave charge floor to 18 regions, evaluate different parameters and their interactions that are assumed to affect the curing process. Then, regression models that relate the curing duration of each area with those parameters are developed. In the second stage, we determine the placement of the products in the autoclave using the regression models of the first stage. We develop a multi-objective nonlinear mixed integer programming model that minimizes the two objectives mentioned above. We linearize this model using additional variables and use ε-constraint method to generate the nondominated frontier. To obtain solutions in shorter durations, we employed one of the well-known multi-objective evolutionary algorithms, Nondominated Sorting Genetic Algorithm-II (NSGA-II). The validity of the practical use of the model is tested on real cases in a composite factory in Turkey.

Key words: Composite, Autoclave, Regression, Multi-objective Layout Optimization, NSGA-II

ÖZET

OTOKLAV İÇERİSİNDE KOMPOZİT PARÇA YERLEŞİMİ OPTİMİZASYONU

Gözdenur KIRDAR

Yüksek Lisans, Endüstri Mühendisliği Bölümü

Tez Danışmanı: Asst. Prof. Dr. Diclehan TEZCANER ÖZTÜRK

Eş Danışman: Prof. Dr. Murat Caner TESTİK

Ağustos 2020, 69 Sayfa

Kompozit parça üretiminde çoğu zaman birden fazla parça tek bir parti halinde otoklava yüklenir. Tipik bir otoklav kür döngüsünün üç ana fazı vardır ve şu şekilde gerçekleşir; ısıtma fazında tüm parçalar kür sıcaklığına ulaşana dek ısıtılır, ardından bekleme fazında parçalar belirli ve sabit bir süre bu sıcaklıkta bekletilir ve son olarak soğuma aşamasında parçalar soğutularak kür döngüsü tamamlanır. Bir kür döngüsünde ana hedef tüm parçaların tam olarak kürlenmesidir. İdeal bir kür döngüsünde, tüm parçalar aşırı kürlenmeden kaçınarak aynı zamanda kür sıcaklığına ulaşır. Fakat bu şartı sağlamak parça konumlarına, geometrilerine, yüklemedeki toplam kütleye, vb. faktörlere bağlı olarak çoğu zaman mümkün olmamaktadır. Kür sıcaklığına ulaşan ilk parça (önden giden), son parçanın (geciken) kür sıcaklığına ulaşması için gereken süre farkı kadar fazla kürlenir. Bu zaman farkı, kür döngüsü sırasında tüm parçalar üzerindeki termokuplar ile izlenebilir ve ürün kalitesini büyük ölçüde etkiler. Bu gecikme en aza indirilirse, daha kaliteli ürünler üretilebilir. Bir diğer husus, ısıtma aşamasını kısaltarak toplam proses süresinin en aza indirilmesidir. Bu şekilde zaman ve enerji tasarrufu elde edilebilir.

Bu çalışmada hem parçalar arasındaki zaman gecikmesini hem de ısıtma fazının süresini en aza indirmek için iki aşamalı bir yaklaşım geliştirdik. İlk aşamada, kür sıcaklığına ulaşma süresini etkileyen faktörleri belirledik. Otoklav şarj tabanını 18 bölgeye ayırdık ve kürleme sürecini etkilediği varsayılan farklı parametreleri ve bunların etkileşimlerini değerlendirdik. Ardından her bir alanın kürlenme süresini bu parametrelerle ilişkilendiren regresyon modelleri geliştirdik. İkinci aşamada, ürünlerin ilk aşamadaki regresyon modellerini kullanarak otoklavdaki yerleşimini belirledik. Yukarıda belirtilen iki hedefi en aza indiren doğrusal olmayan karma bir tamsayılı programlama modeli geliştirdik. Bu modeli ek değişkenler kullanarak doğrusallaştırdık ve etkin çözümleri ε-kısıt yöntemi ile bulduk. Daha kısa sürelerde çözüm elde etmek için yaygın kullanılan çok amaçlı evrimsel algoritmalardan birini, Nondominated Sorting Genetic Algorithm-II (NSGA-II), kullandık. Modelin pratik kullanımının geçerliliğini Türkiye'deki bir kompozit fabrikadaki gerçek durumlarda test ettik.

Anahtar Kelimeler: Kompozit, Otoklav, Regresyon, Çok Kriterli Yerleşim Optimizasyonu, NSGA-II

ACKNOWLEDGEMENTS

I would like to express my sincere gratitude to my academic advisors, Asst. Prof. Dr. Diclehan TEZCANER ÖZTÜRK and Prof. Dr. Murat Caner TESTIK for the continuous support of my M.Sc. study and research, for their patience, motivation, enthusiasm, and immense knowledge.

Besides my advisors, I would like to thank all my professors and administrative staff who have worked in the Department of Industrial Engineering at Hacettepe University.

CONTENTS

FIGURES

TABLES

SYMBOLS AND ABBREVIATIONS

Symbols

P_i	Weight of part i
L_i	Length of part i
W_i	Width of part i
ρ	Small positive number
M	Large positive number
β_{jl}	l^{th} Regression coefficient of area j including no f interactions
β_{ju}	u^{th} Regression coefficient of area j including f interactions
c_{il}	l^{th} Regression value of part i
d_{iu}	uth Regression value of part i
$\bar{c}_{jl}$	Average of the observed values of predictor variable l ∈ L in area j
$\bar{d}_{ju}$	Average of the observed values of predictor variable u ∈ U in area j that is made of the terms not including F
$\bar{f}_j$	Average of the observed values of front part weights in area j
x_{ij}	= 1, if part i is placed in area j; 0, otherwise
f_j	Total part weight in front of area j
e_{iju}	Factor for part i which have front parts
t_{lead}	Time to reach curing temperature of leading part
t_{lag}	Time to reach curing temperature of lagging part
t_i	Time to reach curing temperature of part i
P_t	Initial population at generation t
Q_t	Offspring population at generation t
R_t	Combination of initial population and offspring population at generation t
F_n	Front number

Abbreviations

HVI	Hyper-volume Indicator
MOMILPM	Multi-objective Mixed Integer Linear Programming Model
NSGA-II	Nondominated Sorting Genetic Algorithm-II
MOEA	Multi-objective Evolutionary Algorithm
VIF	Variance Inflation Factor

1. INTRODUCTION

In recent years, with the increasing number of studies on composite technologies, aluminum and metal materials are increasingly being replaced by composite materials due to their low density, high corrosion resistance and design flexibility. After Boeing and Airbus announced in 2010 that the materials used in the production of 787 Dreamliner and Airbus A350XWB were about 50% by weight composite, aircraft manufacturers have begun to give more importance to this field and almost all of them have added some kind of composite material to their new aircraft designs[1]. As well as civilian and military airplanes, with the increasing applications in defense industry, composite materials have been started to be used in military aircrafts such as helicopters, armored vehicles such as tanks, panzers, heavy vehicles used in military transportation, bulletproof vests, and weapon bodies[2].

In composite industry, pre-impregnated carbon, glass or aramid fibers impregnated with resin are called prepregs. Prepreg fibers are generally processed by autoclave method. In this method, the prepreg layers are placed on top of each other over a lay-up mold by a technician. Then, this group of composite parts (whole of molds and prepregs) with similar curing properties are put into the pressurized oven called autoclave together in batches. The aim is to heat all materials up to the curing temperature (that is common for all parts put together), stay at that temperature for a certain duration (the dwell period), and then cool all parts by lowering the autoclave temperature and pressure. As a process rule, the dwell period starts after all parts reach the curing temperature. In general, it is often not possible for all parts to reach the curing temperature simultaneously. Reaching this temperature depends on the locations of the parts in the autoclave charge floor since the parts closer to the hot gas source heats up faster that the distant ones. In addition to distance, another important factor is the relative positioning of the parts in the autoclave due to forced convection. Total batch weight, individual part weight and size are also considered as important factors in this study since mass and shape play important roles in heat transmission.

For a part, the time interval between the instant it reaches the curing temperature and the start of the dwell period is called delay. This has impact on product quality as the parts

that reach the curing temperature earlier than the others wait for the others, while they are overexposed to that temperature. This, in turn, worsens their product quality. Dwell period is defined by the customer and cannot be changed. All parts must be cured during this time interval. Also, due to the amount of energy that an autoclave consumes, the autoclave curing process is quite expensive. However, it is possible to reduce the total processing time by shortening the heat-up and cool-down periods without changing the dwell period. For heat-up period, if all parts reach the curing temperature earlier, the process time gets shorter. This provides a considerable amount of time and energy saving and better quality.

Considering these three important effects; time, cost and quality, the main objectives of this study are to minimize both the heat-up period and the maximum delay of the parts, by arranging the part placements in the autoclave charge floor. For this purpose, we divide the autoclave charge floor into 18 rectangular areas and develop a multiple regression model for each area that predicts the time to reach the curing temperature. For these models, we use the data collected in 2017-2018 for 23 different parts from 3 different families. Then, using the regression models, we develop a MOMILPM that minimizes both the heat-up period and the maximum delay of the parts. We employ ε-constraint method to determine the efficient solutions. To decrease the computational burden further, we use NSGA-II to approximate the nondominated frontier. We test our approach using real cases in a composite factory in Turkey.

Following shows the thesis' structure; Chapter 2 presents the literature survey about autoclave process optimization. Chapter 3 introduces the problem definition. Chapter 4 focuses on our solution approach. Chapter 5 discusses the results. Ultimately, Chapter 6 contains the conclusions and some further study.

2. LITERATURE REVIEW

There are many studies in the literature on curing process for composite parts. Some studies are about improving heat transfer via mold design and layout. Wang et al.[3] have presented a method for uniform heating of the mold. They have also numerically investigated the curing efficiency of curved composite parts based on thermal gradients of molds[4]. Jian Hu et al.[5] have proposed another method for uniform heating of the mold by using a "heat conducting fin". Haskilic[6], on the other hand, have developed a MILPM for autoclave loading and scheduling.

To the best of our knowledge, the literature on autoclave parts placement is quite scarce. One of the most recent studies on a similar subject has been done by Maffezzoli and Grieco[7]. Similar to our problem, their aim is to optimally locate different tools inside the autoclave minimizing the delay function. To do that, they have developed an assignment model, where each tool-location assignment has a penalty that depends on the thermal characteristics of the parts, their horizontal and vertical positions, and their shadow effects. With this method, delay time can be found for each piece. Their method is valid for a certain type of autoclave and the problem is modelled over parts. Also, the penalty coefficient is studied as a function of the absolute position, ignoring the effect of the other tools, and of the relative position considering for the effect of the close parts. As a result, they have achieved a significant reduction in the cure time after simulating behavior of three real autoclave batches.

Unlike the model offered by Maffezzoli and Grieco[7], taking into account the coordinates and orientation of the part, Dios et al.[1] have proposed a more general model that can be used in different autoclaves. They have approached the problem as a two-dimensional Bin Packing Problem based on the container-loading model by Chen et al.[8] and developed a MILPM by using penalties introduced in Maffezzoli and Grieco[7]. They test their model using the scenarios given in [7] and achieved better results.

In another study by Nele et al.[9], a parameter, S, based on the geometry of the part-mold combination and thermal inertia has been determined in order to find the optimal position to minimize maximum delay in the heat-up and cool-down periods for the entire batch. They propose putting parts with larger S values closer to the door.

As seen, in the literature, the studies on optimization of the curing time of the parts in the autoclave are very limited due to the fact that autoclave process highly depends on autoclave type and the parts assigned to it. In our study, we also employ a problem-

specific approach. We address the parts placement problem for an autoclave that is capable of curing 18 parts simultaneously. We divide the autoclave charge floor into 18 areas and predict the curing time of each of the areas, while other studies in the literature predict the curing time by modelling over parts. Also, we consider two conflicting objectives in deciding on the placements that none of the studies have considered.

Given 18 areas and 18 products, our problem can be categorized as a Facility Layout Problem which optimally finds the placement of the composite parts in the autoclave so that the time difference between leading (the part that reaches the curing temperature first) and lagging (the part that reaches the curing temperature the latest) parts and the heat-up period are minimized. By this minimization, it is expected to have more efficient operations and better quality in addition to less manufacturing costs and shorter lead times[10]. The layout problems are addressed via exact or approximated approaches as given in Figure 2.1. In this study, we employ ε-constraint method to find all efficient solutions, and NSGA-II to approximate these efficient solutions.

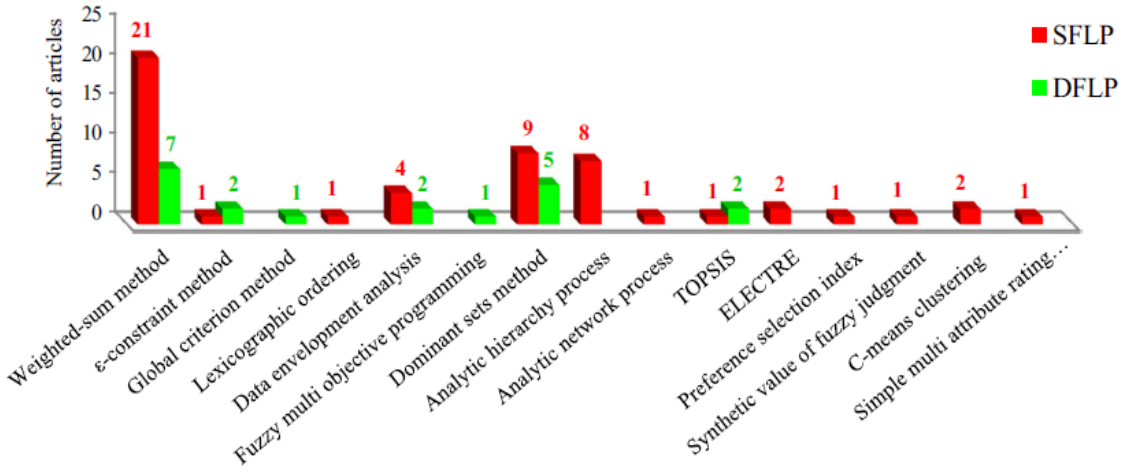

Figure 2.1 Methods for Solving Multi-Criterion FLPs [11]

3. PROBLEM DEFINITION

3.1. Autoclave Curing Process

The autoclave used in this study is heated via nitrogen. It has an internal length of 275 inch and a diameter of 98 inch as given in Figure 3.1. It utilizes H-Slot air flow adjustment panels at the door side to balance air flow in the autoclave. H-slot adjusters provide evenly distributed, turbulent flow in 100% of the working area and allow uniform heating and cooling of the part load. This type of autoclave incorporates floor-mounted heaters and cooling radiators. The fan is located at the back of the autoclave. The gas in the autoclave is transferred from the rear of the autoclave to the front via floor duct by passing floor-mounted heater or cool radiator. Then the gas meets with H-Slot panels at the door and goes towards rear of the autoclave. This circulation continues through the process. This autoclave is a typical industrial autoclave in which composite parts are subjected to a temperature/pressure cycle known as the "process cycle" in order to cure the matrix resin, accomplish ideal fiber and resin distribution and to minimize the void content. The quality of the parts profoundly depends on this cycle; hence it is important that all perspectives of the cycle is planned well. The process is carried through three periods; heat-up, dwell and cooling as depicted in Figure 3.2. In the heat-up period, both temperature and pressure increase. When all parts reach the curing temperature, dwell period starts and the parts are maintained at this temperature for a defined period of time so that polymerization takes place. At the end of this period, cooling phase begins and the temperature and pressure decrease until the defined values to open autoclave door safely.

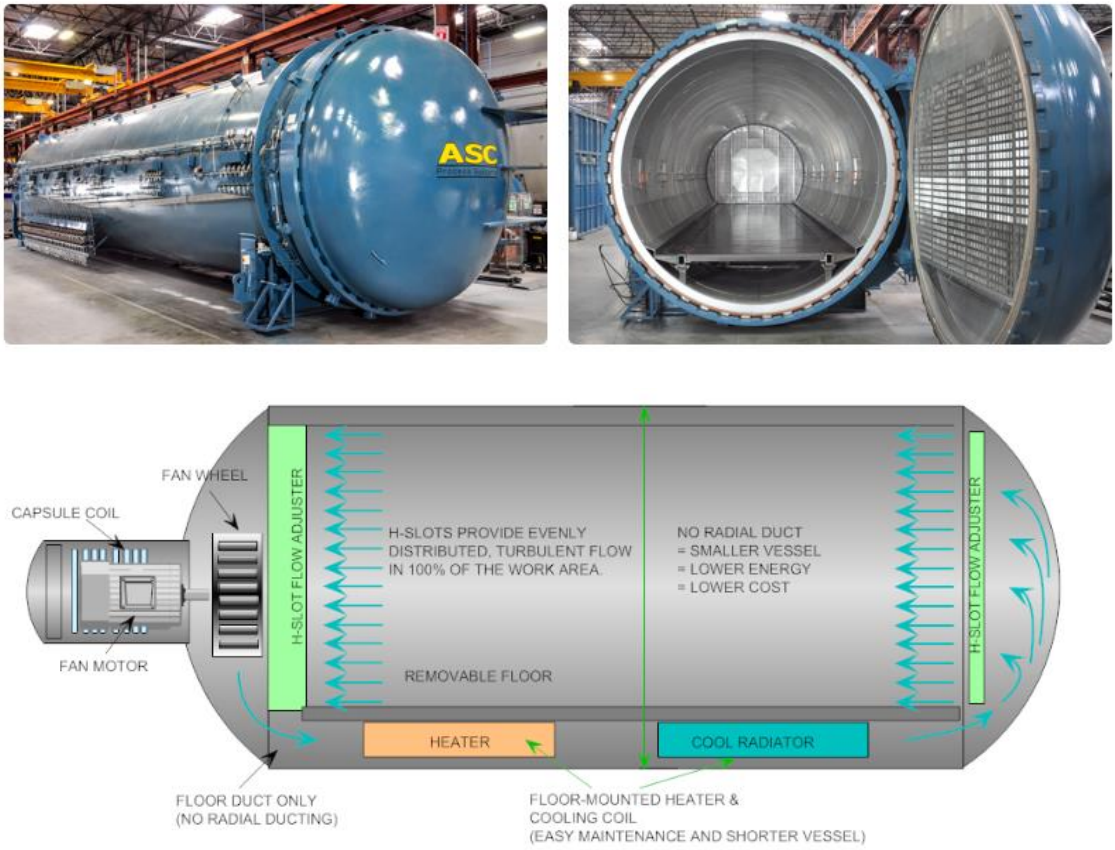

Figure 3.1 Picture and Sketch of Studied Autoclave

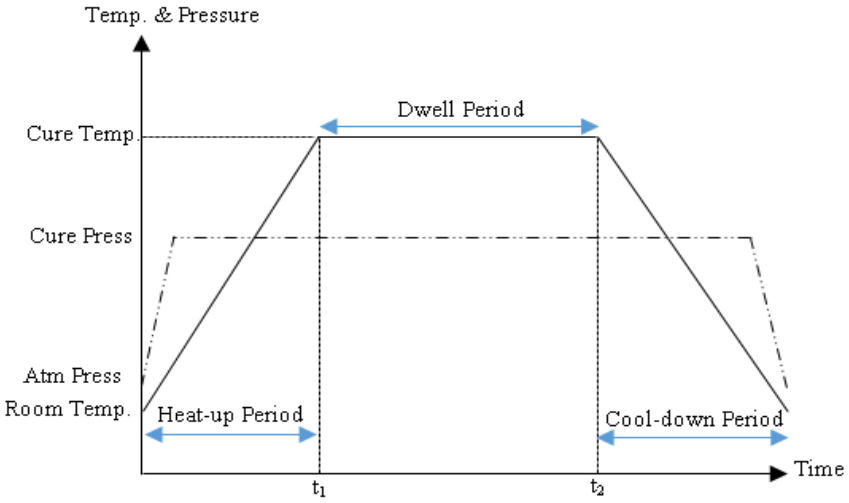

Figure 3.2 Autoclave Curing Cycle Stages

3.2. Parts Loaded in the Autoclave

The process parameters given in the recipe is controlled by a software, "Composite Processing Control", via thermocouples and pressure sensors during a cure cycle. It has 36 thermocouples to record the temperature of the parts loaded in the autoclave and 12 pressure sensors to monitor the pressure on the parts. As a process rule, there should be 2 thermocouples located on each part to prevent data losses in case one thermocouple becomes disabled during the curing cycle. So, maximum number of parts that can be cured together in one cycle is 18. The locations of the thermocouples on the parts are decided with customer during preproduction verification step.

The products used in our experimental studies belong to 3 families namely; 9 parts from Family A, 2 parts from Family B and 16 parts from Family C and their basic features are given in Table 3.1. The families consist of different parts in size but they have common fabrication features.

Table 3.1 Basic Features of the Parts

Family	Part Contour	Material	Tool Material	Number of Parts	Weight (lb)	Width (inch)	Length (inch)
A	Complex Curvature	-Prepreg Carbon Fiber -Honeycomb Core -Adhesive Film -Tedlar Film	ST52-Steel	9	128-208	14-17	37-67
B	Flat	-Prepreg Carbon Fiber	ST52-Steel	2	183	8	70
C	Flat	-Prepreg Carbon Fiber	ST52-Steel	16	16-31	10-12	10-15

3.3. Planning the Autoclave Cure Cycle

In the autoclave curing cycle, one of the most critical steps for final laminate properties is reaching and maintaining at the curing temperature. In the ideal case, all parts reach this temperature at the same time and none is exposed to additional heating. However, it is almost not possible for all parts to reach the curing temperature at the same time in one autoclave cycle. Delays between parts usually occur. To understand delay, let's consider an autoclave process with a curing temperature of 170^{o}C and a dwell period of 150 minutes. We may assume that part A is the leading part (the part that reaches the curing

temperature the first) that reaches the curing temperature in 100 minutes and part B is the lagging part (the part that reaches the curing temperature the latest) that reaches the curing temperature in 120 minutes. Then, the dwell period starts at the 120th minute for both. Thus, instead of remaining at the curing temperature for 150 minutes, part A remains at there for 170 minutes and is over-cured for 20 minutes. This over-cure duration worsens the quality of part A.

Another important consideration is the duration of the overall autoclave curing cycle. If the curing cycle is shortened, the process becomes more time-efficient and less costly. For example, considering that this autoclave works 3 times a day for an average of 7 hours for each run, and that 1 hour is reserved for set-up in total, even achieving a 10-minute improvement in the total working time will allow 1 extra run in 2 weeks. Among the three periods, dwell period's duration cannot be changed since it is determined by the customer. However, if all products reach the curing temperature earlier, the heat-up period can be shortened.

Both the quality of the final products and cost/time efficiency of the cure cycle are affected by the duration that each part reaches the curing temperature. This duration is mainly affected by how the parts are placed in the autoclave. For example, in the past data, there are three different layouts that the same 18 parts are placed previously, and all parts' temperature values during the curing cycle were recorded. The heat-up period durations are 27.5, 63.0 and 25.4. The maximum delay values for the corresponding layouts are 127.1, 139.3 and 130.1. The only difference between those curing processes is how the parts are placed in the autoclave. In our study, we consider two objectives while determining the parts placement in the autoclave: minimization of heat-up period, and minimization of maximum delay to reach the curing temperature. For our case, there are no relations established between the time to reach the curing temperature and how the part is placed. In our approach, we first develop the relation between the time to reach the curing temperature and how the product is placed. Using this relation, we then find efficient placements of parts that consider both of the objectives.

We explain our two-stage solution approach in Section 4. In the first stage, we develop the relation between the time to reach the curing temperature and how the product is placed with respect to the other products. We first determine the factors that may affect the time to reach the curing temperature. Mass and shape play important roles in heat

transmission, in addition to location, total batch weight, individual part weight and size were also considered as important factors in this work. Using multiple regression models, we relate these factors with the time to reach the curing temperature. In the second stage, we use this relation to find efficient placements of a group of parts in the autoclave that optimizes the two objectives. We first develop a nonlinear mixed integer programming model which is then linearized. Using this linear model, we find the efficient placements. We also employ a multi-objective evolutionary algorithm to approximate these efficient solutions in case good solutions are required in shorter durations.

4. SOLUTION APPROACH

In this section, we explain our two-step solution approach.

4.1. Phase 1: Estimating the Time to Reaching Curing Temperature

We first evaluate the effect of location on the time to reach the curing temperature. We divide the autoclave charge floor into 18 areas as in Figure 4.1. The length and the width are divided to 6 and 3 equal-length grids, respectively. The reason for dividing it into 18 areas is that the autoclave capacity is 18 parts at most and each rectangular area is in the most suitable form for loading in terms of shape of the parts by this approach. Additionally, in the previous data, there were sketches of the part placements in the autoclave. Although the autoclave floor was not divided to 18 areas explicitly, with our division, all parts fit in one of these areas suitably. We examined 705 data including part name, location, thermocouple readings according to time, coming from 62 separate runs of 27 different parts belonging to 3 different families with respect to their areas. We grouped the data with respect to the area the product is put. Average times of reaching curing temperature according to areas are given in Figure 4.2. It is obvious that location has a considerable effect on timing as having similar trend in reaching the curing temperature when parts are put in the same area. It also shows that curing time gets longer as we move from back side to front side of the autoclave. This is unexpected because the temperature is higher at the door side. However, this proves that location is not the only variable that affects the curing temperature. Therefore, we decided to build a regression model for each of the 18 areas to estimate the time to reach the curing temperature by using extra factors in addition to location.

FAN SIDE		
1	7	13
2	8	14
3	9	15
4	10	16
5	11	17
6	12	18
DOOR SIDE		

Figure 4.1 Autoclave Charge Floor Layout

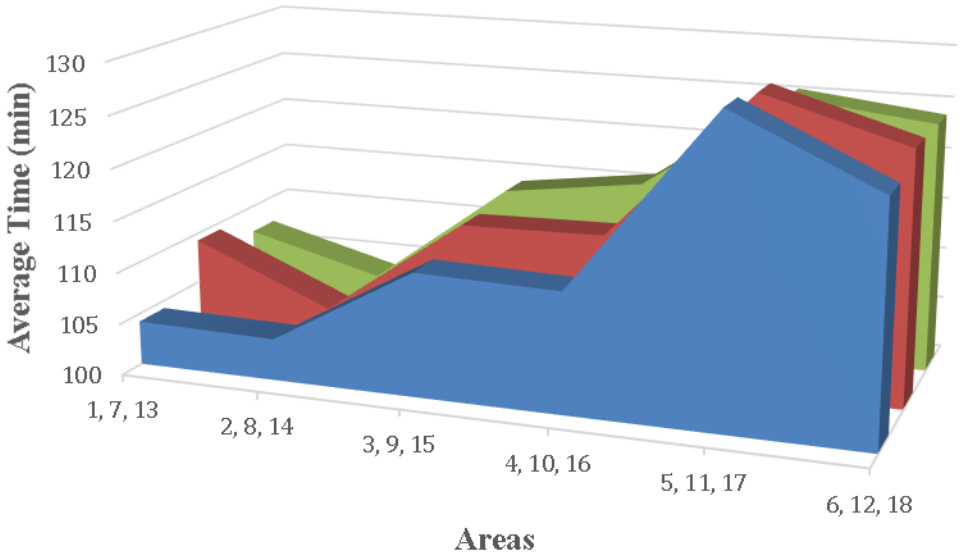

Figure 4.2 Average Time to Reach Curing Temperature for Each Area

The factors that we consider as important in the regression model are weight of the parts in front of each part (towards the door) (F), total batch weight (B), individual part weight (P), length of the part (L) and width of the part (W). Consider an example layout given in Figure 4.3. The total batch weight, B, is the sum of the weights of all parts. The other measure, F, depends on the area the part is placed. For instance, the total weight in the front of area 1, F_1, is calculated by summing the weights of all parts in areas 2 and 3. Here, note that, we allow at most two parts to be placed in one area.

$B= P_1+P_2+P_3+P_4+P_5+P_6+P_7+ P_8+P_9+ P_{10}+P_{11}+ P_{12}$

$F_1= P_2+P_3+P_4+P_5$

$F_5= P_9$

FAN SIDE		
Area 1 Part 1	**Area 4** Part 6	**Area 7** Part 10
Area 2 Part 2 | Part 3	**Area 5** Part 7 | Part 8	**Area 8** Part 11
Area 3 Part 4 | Part 5	**Area 6** Part 9	**Area 9** Part 12
DOOR SIDE		

Figure 4.3 Layout Example

4.1.1. The Multiple Regression Models

As explained above, we develop regression models for each of the 18 areas. Our response variable is the time to reach the curing temperature, and our predictor variables are weight of the parts in front of each part (F), total batch weight (B), individual part weight (P), length of the part (L) and width of the part (W).

We next need to determine the variables to include in the area regression models and whether we need to model interactions between those variables. While doing this, attention was paid to determine models with neither more nor less predictors than necessary[13].

For this purpose, Minitab provides different methods to choose the significant predictor variables. Among these methods, stepwise regression is used in this study. According to this method, in each step, it is decided whether a variable should remain in the model or be discarded depending on predefined criterion[14]. This strategy was utilized including second order terms un-hierarchically. For example, if A, B and C are selected as predictors, the two-way interactions A*B, A*C, B*C are also tested and the best subset among them is chosen. In an un-hierarchical model, it is not necessary for lower-order terms to be included in the model. To illustrate, a model that includes variable A*B*C does not need to include the variables: A, B, C, A*B, A*C, and B*C. We have chosen to use this method to keep the models as simple as possible, preventing having too many terms in the model.

With a significance level of 0.10, the following regression models for 18 areas are obtained via Minitab. In obtaining the regression models, we used "*subtract the mean*" method in which after calculating the mean for a variable, this mean is subtracted from each observed value of the variable.

$$T_1=\beta_{1,0} + \beta_{1,1}(B-\bar{B}_1)+ \beta_{1,2}(P-\bar{P}_1) + \beta_{1,3}(L-\bar{L}_1)^2$$

$$T_2=\beta_{2,0}+\beta_{2,1}(L-\bar{L}_2) + \beta_{2,2}(P-\bar{P}_2)\,(L-\bar{L}_2) + \beta_{2,3}(P-\bar{P}_2)\,(W-\bar{W}_2)$$

$$T_3=\beta_{3,0}+\beta_{3,1}\,(L-\bar{L}_3) + \beta_{3,2}(B-\bar{B}_3)^2 + \beta_{3,3}(P-\bar{P}_3)\,(L-\bar{L}_3)$$

$$T_4=\beta_{4,0}+ \beta_{4,1}(P-\bar{P}_4) + \beta_{4,2}(W-\bar{W}_4) + \beta_{4,3}(F_4-\bar{F}_4)(W-\bar{W}_4)$$

$$T_5=\beta_{5,0}+\beta_{5,1}(B-\bar{B}_5)+ \beta_{5,2}(F_5-\bar{F}_5) + \beta_{5,3}(P-\bar{P}_5)\,(W-\bar{W}_5)+ \beta_{5,4}(W-\bar{W}_5)\,(F_5-\bar{F}_5)$$

$$T_6=\beta_{6,0} + \beta_{6,1}(P-\bar{P}_6)$$

$$T_7=\beta_{7,0}+ \beta_{7,1}(B-\bar{B}_7)+\beta_{7,2}(F_7-\bar{F}_7)+\beta_{7,3}(B-\bar{B}_7)\,(F_7-\bar{F}_7)$$

$T_8=\beta_{8,0}+\beta_{8,1}(P-\bar{P}_8)+\beta_{8,2}(P-\bar{P}_8)^2+\beta_{8,3}(W-\bar{W}_8)(L-\bar{L}_8)$

$T_9=\beta_{9,0}+\beta_{9,1}(L-\bar{L}_9)+\beta_{9,2}(W-\bar{W}_9)(L-\bar{L}_9)+\beta_{9,3}(B-\bar{B}_9)^2$

$T_{10}=\beta_{10,0}+\beta_{10,1}(B-\bar{B}_{10})+\beta_{10,2}(W-\bar{W}_{10})+\beta_{10,3}(B-\bar{B}_{10})(P-\bar{P}_{10})+\beta_{10,4}(B-\bar{B}_{10})(W-\bar{W}_{10})$

$T_{11}=\beta_{11,0}+\beta_{11,1}(B-\bar{B}_{11})+\beta_{11,2}(W-\bar{W}_{11})(F_{11}-\bar{F}_{11})$

$T_{12}=\beta_{12,0}+\beta_{12,1}(B-\bar{B}_{12})+\beta_{12,2}(W-\bar{W}_{12})+\beta_{12,3}(L-\bar{L}_{12})^2$

$T_{13}=\beta_{13,0}+\beta_{13,1}(P-\bar{P}_{13})+\beta_{13,2}(L-\bar{L}_{13})^2$

$T_{14}=\beta_{14,0}+\beta_{14,1}(B-\bar{B}_{14})+\beta_{14,2}(L-\bar{L}_{14})+\beta_{14,3}(W-\bar{W}_{14})+\beta_{14,4}(L-\bar{L}_{14})^2+\beta_{14,5}(B-\bar{B}_{14})(W-\bar{W}_{14})$

$T_{15}=\beta_{15,0}+\beta_{15,1}(P-\bar{P}_{15})+\beta_{15,2}(W-\bar{W}_{15})+\beta_{15,3}(P-\bar{P}_{15})^2+\beta_{15,4}(B-\bar{B}_{15})(F_{15}-\bar{F}_{15})+\beta_{15,5}(L-\bar{L}_{15})(W-\bar{W}_{15})$

$T_{16}=\beta_{16,0}+\beta_{16,1}(P-\bar{P}_{16})+\beta_{16,2}(B-\bar{B}_{16})^2+\beta_{16,3}(P-\bar{P}_{16})^2+\beta_{16,4}(F_{16}-\bar{F}_{16})(P-\bar{P}_{16})$

$T_{17}=\beta_{17,0}+\beta_{17,1}(P-\bar{P}_{17})$

$T_{18}=\beta_{18,0}+\beta_{18,1}(P-\bar{P}_{18})$

Where T is the time to reach the curing temperature in the j^{th} area, $\beta_{j,r}$ is the r^{th} coefficient of regression model of j^{th} area, B is the total batch weight, P is the part weight, W is the part width, L is the part length, F_j is the total weight of all materials put in front of the j^{th} area until the door, and $\bar{x}_j$ indicates the average of the observed values of predictor variable x in area j.

For the areas 2, 6, 8, 13, 17, 18 the time to reach the curing temperature only depends on the properties of the material placed in that area, while for the remaining areas, it depends on both the part and the parts in / around it. In total, we have 16 different predictor variables. We divide these variables to two, depending on whether they include a variable with term F or not as explained in Section 4.6. We give the regression coefficients of the predictor variables that do not include the term F in Table 4.1, and that include F in Table 4.2.

Table 4.1 Regression Coefficients of Variables without F Term

Variable / Area	1	2	3	4	5	6	7	8	9	10	11	12	13
	Constant	B	P	W	B^2	L^2	L	$B*W$	$B*P$	P^2	$P*L$	$P*W$	$W*L$
1	99.39000	0.01690	-0.18720	-	-	0.02008	-	-	-	-	-	-	-
2	100.41000	-	-	-	-	-	-0.64000	-	-	-	0.01165	-0.06240	-
3	100.51000	-	-	-	0.00001	-	-0.71310	-	-	-	0.00477	-	-
4	114.91100	-	-0.09020	-2.81700	-	-	-	-	-	-	-	-	-
5	129.10000	0.00555	-	-	-	-	-	-	-	-	-	0.02006	-
6	129.68800	-	-0.18490	-	-	-	-	-	-	-	-	-	-
7	168.30000	-0.06710	-	-	-	-	-	-	-	-	-	-	-
8	99.28000	-	-0.13520	-	-	-	-	-	-	0.00159	-	-	-0.08000
9	105.81000	-	-	-	0.00003	-	-0.74940	-	-	-	-	-	-0.07180
10	109.19000	-0.00861	-	-5.84800	-	-	-	-0.00651	0.00022	-	-	-	-
11	129.14000	0.00711	-	-	-	-	-	-	-	-	-	-	-
12	125.86800	0.00890	-	-1.25700	-	-0.02648	-	-	-	-	-	-	-
13	92.89000	-	-0.09950	-	-	0.02839	-	-	-	-	-	-	-
14	136.10000	0.04440	-	1.20000	-	0.02564	-2.64500	-0.00253	-	-	-	-	-
15	104.69000	-	-0.15120	-1.11000	-	-	-	-	-	0.00174	-	-	-0.06140
16	114.94000	-	-0.25920	-	-0.00002	-	-	-	-	0.00097	-	-	-
17	129.61000	-	-0.20800	-	-	-	-	-	-	-	-	-	-
18	128.30000	-	-0.13680	-	-	-	-	-	-	-	-	-	-

Table 4.2 Regression Coefficients of Variables with F Term

Variable / Area	1	2	3	4
	F	$F * B$	$F * P$	$F * W$
1	-	-	-	-
2	-	-	-	-
3	-	-	-	-
4	-	-	-	-0.01877
5	0.22220	-	-	0.13970
6	-	-	-	-
7	-0.28850	0.00026	-	-
8	-	-	-	-
9	-	-	-	-
10	-	-	-	-
11	-	-	-	0.22780
12	-	-	-	-
13	-	-	-	-
14	-	-	-	-
15	-	0.00008	-	-
16	-	-	0.00028	-
17	-	-	-	-
18	-	-	-	-

4.1.1.1. Assumptions

Linear Relationship: The assumption of linear association between the response variable and the predictor variables is first checked by the scatter plots given in Appendix A. All relations are assumed to be monotonic. We next checked the relation via Spearman's correlation. It gives an idea about the power of relationship between two variables. The coefficient (r_s) takes values between +1 and -1 and it shows a strong association as it approaches 1, a weak association around 0.

The r_s values are given in Table 4.3. Although we have a few variables as defined "weak" which are still acceptable, in general, the r_s values indicate that there are moderate or strong relations between variables for most of the areas. The p-values given in the third column of the table also show that there is monotonic correlation for all variable pairs for 0.05 significance level, rejecting the null hypothesis; "H_0: There is no relationship between the two variables."

Table 4.3 Spearman's Correlation Coefficient and P-value of Variables

10,5	Variable	r_s	p-values
Area 1	B	-0.6	0.05
	P	-0.8	0.00
	$L * L$	-0.7	0.01
Area 2	L	-0.7	0.00
	$P * L$	-0.7	0.00
	$P * W$	-0.8	0.00
Area 3	L	-0.8	0.00
	$B * B$	-0.7	0.00
	$P * L$	-0.8	0.00
Area 4	P	-0.7	0.00
	W	-0.8	0.00
	$W * F$	-0.6	0.00
Area 5	B	0.2	0.05
	F	0.3	0.00
	$P * W$	-0.3	0.02
	$W * F$	0.3	0.01
Area 6	P	-0.4	0.00
Area 7	B	-0.7	0.05
	F	-0.7	0.05
	$B * F$	-0.4	0.04
Area 8	P	-0.5	0.03
	$P * P$	-0.5	0.03
	$W * L$	-0.6	0.01
Area 9	L	-0.7	0.00
	$W * L$	-0.7	0.00
	$B * B$	-0.6	0.00

	Variable	r_s	p-values
Area 12	B	0.3	0.01
	W	-0.3	0.01
	$L * L$	-0.3	0.01
Area 13	P	-0.7	0.00
	$L * L$	-0.4	0.01
Area 14	B	-0.4	0.04
	W	-0.8	0.00
	L	-0.5	0.01
	$L * L$	-0.5	0.01
	$B * W$	-0.6	0.00
Area 15	P	-0.7	0.00
	W	-0.7	0.00
	$P * P$	-0.7	0.00
	$B * F$	-0.4	0.03
	$W * L$	-0.8	0.00
Area 16	P	-0.8	0.00
	$B * B$	-0.5	0.00
	$P * P$	-0.8	0.00
	$F * P$	-0.7	0.00
Area 17	P	-0.5	0.00
Area 18	P	-0.4	0.01

Normality: It is checked whether the residuals are distributed normally by checking the normal probability plots given in Appendix A. Except for areas which have few data, mostly, the data points lie on the diagonal line. We therefore assume that the residuals follow a normal distribution.

No Multicollinearity: Polynomial terms or interaction terms may cause multicollinearity. It can be checked via VIF which is the indicator for the power of the relationship between a predictor and the other predictors in the model. It is expected to have VIF value between 1 and 10[15]. VIF values of each predictor variables for all areas are given in Appendix A, in the ANOVA tables. All values are between 1 and 10 so independent variables are not highly correlated with each other.

Homoscedasticity: The residuals should have the similar scatter. Scatterplots of "residuals vs. fits" are checked for homoscedasticity as given in Appendix A. As seen, there are no extreme deviations in the plots, so this assumption is acceptable.

4.1.1.2. Regression Models' Adequacy

To obtain a realistic regression model, while some researchers suggest 10 cases of data for each predictor, some follow a statistical formula to calculate the sample size[15]. Table 4.4 shows the number of variables used and data that we have. From the perspective of nearly 10 cases of data per predictor, data of most of the areas are enough according to the rule. For areas that do not comply with the 10-cases rule, due to data availability, it is assumed that the number of collected data is enough to represent the process.

Table 4.4 Number of Data Collected and Number of Variable

	# of Data	#of Predictors
Area 1	11	3
Area 2	31	3
Area 3	35	3
Area 4	51	3
Area 5	70	4
Area 6	101	1
Area 7	8	3
Area 8	23	3
Area 9	22	3
Area 10	31	4
Area 11	36	2
Area 12	78	3
Area 13	17	2
Area 14	30	5
Area 15	32	5
Area 16	36	4
Area 17	43	1
Area 18	50	1

After that S (the standard error) and R^2 were checked. S and R^2 are the two measures of how well the regression model fits the data. While S represents the absolute measure of the difference between the data and the fitted values, R^2 shows the relative measure of the percentage of the dependent variable variation that the model explains. From this perspective, S is the main indicator to directly assess how well the model describes the response. It is expected that S to be as small as possible. In our study, S is chosen to be acceptable as around 5.

As for R^2, higher R^2 values signifies that regression model is capable of explaining higher percentages of the variation. However, even if additional variables are not significant, including more variables to a regression model may cause the R^2 statistic to increase. For this reason, it is suggested that if there are many variables included in a regression model checking adjusted R^2 can be a more appropriate[16]. It increases only if the added term increases the explanatory power of the model. In addition, predicted R^2 the indicator of overfitting if it is distinctly smaller than R^2 should also be checked.

For goodness-of-fit test, S, R^2, adjusted R^2 and predicted R^2 values are given in Table 4.5. The R^2 and adjusted R^2 values of the areas (5 and 18, and partly areas 6, 11, 12, and 17) are relatively low. A common property of those areas is that they are on the door side and other factors or variables might be affecting their warming, which are not considered in

this study. However, as explained before, R-square is a measure of explanatory power, not fit. So, we can still count on related regression models. As for the areas whose S values are around 7, although dropping nearly 3 outlier data per area due to being obviously measurement error, there may still be outliers in the raw data which should be investigated in detail and discarded. Since data was collected in 2017-2018, there was no chance to investigate the reasons. So, we did not discard any more data. In addition to that, it is seen that predicted R^2 is not distinctly smaller than R^2.

Table 4.5 Goodness-of-fit Statistics

	S	R^2	R^2 (adj)	R^2 (pred)
Area 1	4.8	93.2	90.3	84.0
Area 2	6.6	83.6	81.8	78.8
Area 3	5.6	89.9	88.9	86.2
Area 4	6.3	83.3	82.3	79.2
Area 5	8.2	41.5	37.9	30.5
Area 6	7.5	62.1	61.7	59.6
Area 7	3.8	94.1	89.7	77.4
Area 8	5.5	82.6	79.8	69.0
Area 9	6.6	84.3	81.6	77.18
Area 10	6.5	87.0	85.0	81.1
Area 11	5.1	62.9	60.6	50.8
Area 12	7.4	70.4	69.2	65.6
Area 13	4.7	92.1	91.0	88.4
Area 14	4.6	92.2	90.9	88.3
Area 15	4.7	88.5	86.3	83.5
Area 16	5.9	88.0	86.7	85.9
Area 17	5.3	60.1	59.2	56.3
Area 18	7.4	46.0	44.9	38.6

4.1.1.3. Regression Models' Verification

We evaluated generated regression models by an experiment as given in Section 5. To do that, we defined a new layout and estimated curing times via generated regression models. Then, we tested performance of regression models by comparing the predicted curing times with actual curing times. Table 4.6 shows the comparison of the real times and the estimated times. As seen from the table, our estimation for every part and for the difference is satisfactorily close to the real times. So, it can be said that our models can make accurate predictions.

Table 4.6 Predicted vs. Realized Heat-up Durations (min)

	Predicted T (min)	Realized T (min)	Difference (min)
Part 1	122.95	117.93	5.02
Part 2	122.07	120.98	1.09
Part 3	115.28	111.83	3.50
Part 4	115.41	118.95	-3.54
Part 5	122.95	125.05	-2.10
Part 6	120.62	110.82	9.80
Part 7	112.84	106.75	6.09
Part 8	121.44	120.98	0.46
Part 9	121.72	113.87	7.85
Part 10	121.95	114.88	7.07
Part 11	112.84	108.78	4.06
Part 12	110.78	105.73	5.05
Part 13	114.81	105.73	9.08
Part 14	112.78	106.75	6.03
Part 15	110.78	112.85	-2.07
Part 16	114.03	114.88	-0.86
Part 17	121.06	123.02	-1.99
Part 18	112.44	117.93	-5.49

4.2. Phase 2: Finding the Placement of Parts in the Autoclave

In our second stage, we find the efficient placements of parts to the areas in the autoclave. We decide on which part is placed to which area, while minimizing the two objectives: the duration of the heat-up phase and the maximum delay of the parts.

Before we continue with our solution approach, we give some definitions. The definitions are taken from [12]. Here, let x denote the decision variable vector, X denote the feasible set, Z denote the image of the feasible set in objective function space, and point $z(x)=(z_1(x), z_2(x),\ldots, z_p(x))$ be the objective function vector corresponding to the decision vector x, where p is the number of objectives and $z_k(x)$ is the performance of solution x in objective k. We assume without loss of generality, that all objectives are to be minimized.

Definition 1: A solution $x \in X$ is an efficient solution if there does not exist $y \in X$ such that $z_k(y) \leq z_k(x)$, for at least one k. Otherwise, x is an inefficient solution. The efficient set is made of all efficient solutions.

Definition 2: If x is efficient (inefficient), then z(x) is said to be nondominated (dominated).

We next explain our assumptions in placing a batch of products in an autoclave.

- At most two products can be placed in an area,
- Orientations of all parts in the autoclave are decided by the customer according to the part-mold thermal profile, therefore their orientations are considered as constant,
- The total width of parts placed horizontally can be at most 96 inches,
- The total length of parts placed vertically can be at most 275 inches,
- Maximum 4 parts can be placed next to each other horizontally.

Due to the variables including the term F, our first model is a mixed integer nonlinear program. The parameters and variables used when constructing mathematical model are given as follows:

Sets and Indices

$i \in I = \{1,\dots,18\}$	Set of composite parts
$j,k \in J = \{1,\dots,18\}$	Set of areas in autoclave charge floor
$a \in A = \{1,2,3\}$	Set of vertical divisions in the autoclave
$l \in L = \{1,\dots,13\}$	Set of predictor variables without the term F
$u \in U = \{1,\dots,4\}$	Set of predictor variables including the term F

Parameters

P_i	Weight of part i
L_i	Length of part i
W_i	Width of part i
H	Maximum number of parts that can be placed horizontally in the autoclave
W	Width of the autoclave
L	Length of the autoclave
β_{jl}	Regression coefficient of predictor variable $l \in L$ in area j
β_{ju}	Regression coefficient of predictor variable $u \in U$ in area j
c_{il}	The value of predictor variable $l \in L$ of part i
d_{iu}	The partial value of predictor variable $u \in U$ of part i that is made of the terms not including F; d_{i1}=1, d_{i2}= B, d_{i3}=P_i, d_{i4}= W_i for all $i \in I$
$\bar{c}_{jl}$	Average of the observed values of predictor variable $l \in L$ in area j

$\bar{d}_{ju}$ Average of the observed values of predictor variable $u \in U$ in area j that is made of the terms not including F

$\bar{f}_j$ Average of the observed values of front part weights in area j

Decision Variables

x_{ij} = 1, if part i is placed in area j; 0, otherwise

f_j Total part weight in front of area j

y_j The maximum length of the parts placed in area j

t_{lead} Time to reach the curing temperature for the leading part

t_{lag} Time to reach the curing temperature for the lagging part

t_i Time to reach the curing temperature for part i

Mixed Integer Nonlinear Programming Formulation (Model N)

$$\min z_1 = t_{lag} - t_{lead} \quad (1)$$

$$\min z_2 = t_{lag} \quad (2)$$

Subject to

$$t_i = \sum_{j=1}^{18} x_{ij}[\sum_{l=1}^{13} \beta_{jl}\,(c_{il} - \bar{c}_{jl}) + \sum_{u=1}^{4} \beta_{ju}(d_{iu} - \bar{d}_{ju})(f_j - \bar{f}_j)] \quad \forall\, i \in I \quad (3)$$

$$\sum_{j=1}^{18} x_{ij} = 1 \quad \forall\, i \in I \quad (4)$$

$$\sum_{i=1}^{18} x_{ij} \leq 2 \quad \forall\, j \in J \quad (5)$$

$$\sum_{i=1}^{18} (x_{i,j} + x_{i,j+6} + x_{i,j+12}) \leq H \quad j = 1, \dots, 6 \quad (6)$$

$$\sum_{i=1}^{18} W_i(x_{i,j} + x_{i,j+6} + x_{i,j+12}) \leq W \quad j = 1, \dots, 6 \quad (7)$$

$$y_j + y_{j+1} + y_{j+2} + y_{j+3} + y_{j+4} + y_{j+5} \leq L \quad j = 1,7,13 \quad (8)$$

$$y_j \geq L_i x_{ij} \quad \forall\, i \in I, j \in J \quad (9)$$

$$f_j = \sum_{k=j+1}^{6a} \sum_{i=1}^{18} P_i x_{ik} \quad a \in A,\ j = 6a-5, \dots, 6a-1 \quad (10)$$

$$t_{lag} \geq t_i \quad \forall\, i \in I \quad (11)$$

$$t_{lead} \leq t_i \quad \forall\, i \in I \quad (12)$$

$$x_{ij} \in \{0,1\} \quad \forall\, i \in I, j \in J \quad (13)$$

The model finds the optimal locations of parts to be cured in autoclave and it has two objectives; the first one is minimization of the time difference between leading and lagging parts at reaching curing temperature and the second one is minimization of the heat-up period. The heat-up period ends when all parts reach the curing temperature, so that the part that reaches the curing temperature the latest determines the duration of the heat-up period. Constraint (3) is constructed as above due to using subtract the mean method and it finds the time to reach the curing temperature of each part i The regression coefficient is multiplied with the parameter value of the part that is deduced by the mean of the observed values. Constraint (4) places each part in one area. Constraints (5) and (6) ensure that maximum 2 parts can be in one area and maximum 4 parts can be placed next to each other horizontally, respectively. Constraints (7), (8) and (9) are defined for limitation of autoclave dimension. The total width of parts placed horizontally can be at most W inches, and the total length of parts placed vertically can be at most L inches. Since we can place more than one part in an area, we find the maximum length placed in each area and add those maximum values to restrict by L inches. Constraint (10) calculate the total front weight of each area. Lastly, constraints (11) and (12) are for identifying lagging and leading parts temperature and constraint (13) define the decision variables.
In our model, we set $H = 4$, $W = 98$ and $L = 275$.

Model *N* is a nonlinear model due to constraint (3) that includes the multiplication of decision variables x_{ij} and f_j. We thus convert it to an equivalent linear model by defining a new variable e_{iju}. By using e_{iju}, constraint (3) is replaced with constraint (3*) and new constraints (14)-(17) are included. We give the modified formulation below, and the whole formulation in Appendix B for completeness.

Mixed Integer Linear Programming Formulation (Model L)

Min (1)

Min (2)

Subject to

$$t_i = \sum_{j=1}^{18} x_{ij} \sum_{l=1}^{13} \beta_{jl} \left(c_{il} - \bar{c}_{jl}\right) + \sum_{j=1}^{18} \sum_{u=1}^{4} e_{iju} \qquad \forall\, i \in I \qquad (3^*)$$

$$e_{iju} \leq M x_{ij} \qquad \forall\, i \in I, j \in J, u \in U \qquad (14)$$

$$e_{iju} \geq -M x_{ij} \qquad \forall\, i \in I, j \in J, u \in U \qquad (15)$$

$$e_{iju} \leq \beta_{ju}\left(d_{iu} - \bar{d}_{ju}\right)\left(f_j - \bar{f}_j\right) + M(1 - x_{ij}) \qquad \forall\, i \in I, j \in J, u \in U \qquad (16)$$

$$e_{iju} \geq \beta_{ju}(d_{iu} - \bar{d}_{ju})(f_j - \bar{f}_j) - M(1 - x_{ij}) \qquad \forall\, i \in I, j \in J, u \in U \qquad (17)$$

Constraints (14) and (15) ensure that if $x_{ij} = 0$, e_{iju} becomes zero for all predictor variables $u \in U$, and constraints (16) and (17) ensure that if $x_{ij} = 1$, e_{iju} equals $\beta_{ju}(d_{iu} - \bar{d}_{ju})(f_j - \bar{f}_j)$. Here, M is a large positive number.

4.2.1. Generating the Nondominated Frontier

The combinatorial problems can be solved via exact and heuristic methods. The optimal solutions can be found by exact algorithms. However, the run-time usually increases with the problem size. In addition, often up to moderately-sized problems can be solved to optimality. As for larger cases, to get solutions in a shorter time via heuristic algorithms by trading optimal solutions off is quite common[17]. Considering that the autoclave runs three times a day in busy periods, the new layout plans should be obtained as quickly as possible for situations such as changes in the parts to be loaded and due date restrictions. So, due to computational time concerns both an exact method and a heuristic method are proposed in this study as below subsections.

4.2.1.1. ε -Constraint Method

In this study, we find the efficient solutions of Model L by using the ε-constraint method[18]. In this method, all but one objective is transformed to constraints and constrained by an ε value. In our case, time difference between parts while reaching curing temperature was retained as the objective function while t_{lag} was constrained to be less than or equal to a specific value ε. The ε-constraint formulation in this study is given below. Here ρ is a small positive constant, and it is multiplied with the second objective and added to the objective function to guarantee obtaining efficient solutions.

$$\min z_1 = t_{lag} - t_{lead} + \rho * t_{lag}$$

Subject to

(3*) - (19)

$$t_{lag} \leq \varepsilon$$

4.2.1.2. A Heuristic Approach: NSGA-II

NSGA-II procedure [19] is an improved version of NSGA and it employs an elitist principle. The purpose of elitism is the keeping best solutions to the next generations. It also supports the diversity in the population.

The procedure is illustrated in Figure 4.4. It starts with the formation of new population, R_t the union of parent population, P_t and child population, Q_t. Both P_t and Q_t have size of

N. R_t is therefore twice the size of the P_t. Then, every individual is ranked based on its performance regarding the objective function values. The better the performance, the better it is ranked. The ranking occurs in different fronts as F_1, F_2, …, F_n. In next step, the next population, P_{t+1} is created by taking all individuals of the best fronts until the size of the original population is reached. If the last front like F_3 in Figure 4.4 is too big that all individuals can get in the new parent population of the next generation, crowding distance sorting is used to select individuals from the same front. To calculate the crowding distance, the distance between nearest neighbors as given in Figure 4.5 is computed at first. Then the delta is divided by the difference of the maximum and the minimum of the objective values. Lastly, this calculation is added up to already calculated distance for the other objectives. After calculating it, the one with a larger crowding distance is chosen. Then, P_{t+1} is used to create offspring population Q_{t+1}. To do that, members of P_{t+1} are matched two by two so that each member joins to two tournaments. Again, the pairs are compared according to their ranks and crowding distances. At the end of this stage, mating pool is ready for crossover and mutation operators[20].

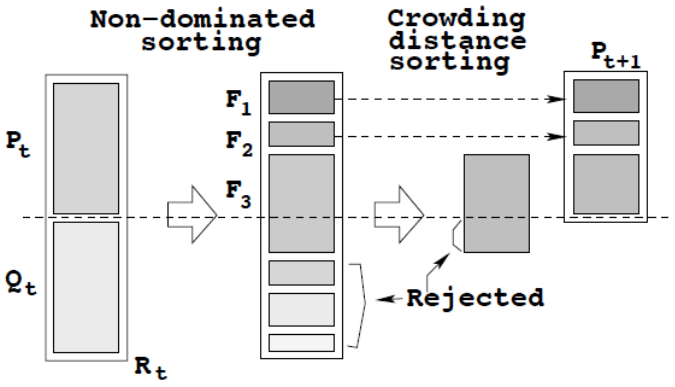

Figure 4.4 Schematic of the NSGA-II Procedure[19]

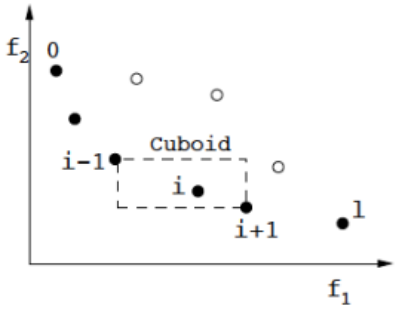

Figure 4.5 The Crowding Distance Calculation [19]

4.2.1.2.1. Development of NSGA-II

4.2.1.2.1.1. Representation and Initial Population

In our study, each chromosome in the population represents a layout and each gene represents the possible area that a part can be put. Due to having at most 18 parts to locate, the length of a chromosome can be at most 18. Each part can be placed to one area in a chromosome, and each area can have at most two parts. To handle these two limitations, we increase the number of possible regions to 36 where two regions correspond to one

area in the original model. For instance, regions 1 and 2 correspond to area 1, regions 3 and 4 correspond to area 2, etc. Each gene is randomly assigned to a number between 1 and 36. An example of an initial population is given Figure 4.6. In the first chromosome, parts 1 and 5 are placed to regions 27 and 28, so that they both are put to area 14. After the initial population is created, each chromosome is subjected to a feasibility check that is explained below.

	1	**2**	**3**	**4**	**5**	**6**	**7**	**8**	**9**	**10**	**11**	**12**	**13**	**14**	**15**	**16**	**17**	**18**
Chr. 1	27	15	31	2	28	11	23	17	34	25	22	30	29	13	18	35	10	21
Chr. 2	10	31	26	27	20	28	17	33	9	13	1	3	14	32	4	30	32	21
Chr. 3	23	14	29	36	5	22	17	6	15	23	10	3	9	18	2	21	28	35
…	…	…	…	…	…	…	…	…	…	…	…	…	…	…	…	…	…	…
…	…	…	…	…	…	…	…	…	…	…	…	…	…	…	…	…	…	…
…	…	…	…	…	…	…	…	…	…	…	…	…	…	…	…	…	…	…
Chr. N	18	30	9	8	10	25	32	23	34	29	10	31	20	3	11	17	15	26

Figure 4.6 An Example of Initial Population Structure

4.2.1.2.1.2. Feasibility Check

In the chromosome, each part is located to one of 36 regions, satisfying constraint (4). As for the remaining constraints (5), (6), (7), (8), we check whether any of them is violated through the following steps.

Check 1. Check all regions whether they contain maximum 2 parts.
Check 2. Check each row whether the sum of the number of the parts in a row is lower than or equal to 4.
Check 3. Check each row whether the sum of the width of the parts in a row is lower than or equal to 96 inches.
Check 4. Check each column whether the sum of the maximum lengths is lower than or equal to 275 inches.

If for a chromosome any of the constraints are violated, we employ two different methods. Our first method is a penalty approach in which if any of the constraints is violated, a cost is added to both of the fitness values. By this, the chromosome which violates at least one constraint takes very high fitness values and its selection becomes less likely after sorting.

Our second method is repair approach. This repair algorithm is applied when new solutions are created (after initial population and mutation in every generation) to check above statements. After each check, if the constraint is violated, the solution is modified to satisfy that violated constraint. First constraints (5) and (6) are checked because it is easier to protect the original chromosome string and it is possible to automatically satisfy

the other constraints (7) and (8) by satisfying constraints (5) and (6). So, we start with Check 1 and if it is provided by all of the areas, we continue with Check 2 and so on. If any violation is detected in one of the checks, it repairs all violations for that constraint, then continues with next check. After all repairs, it runs all checks again until there is no violation left.

To illustrate, a string is given in Table 4.7. As explained before, each area consists of two regions. In terms of constraint (5), there is no problem to locate maximum two parts into one area. However, locating two parts into one region causes violation. In this example, Parts 6, 12 and 16 are assigned to the same region. Also, in the solution in Table 4.7, Parts 15 and 18 are also violating constraint (5) because they are in Area 1 since both are assigned to Region 1. This situation is quite possible because while there is no chance to locate more than one part in the same region in the initial population generation stage, there is a chance to share same region by more than one part after crossover or mutation.

Table 4.7 Area and Region Representation of a Layout

Parts	**1**	**2**	**3**	**4**	**5**	**6**	**7**	**8**	**9**	**10**	**11**	**12**	**13**	**14**	**15**	**16**	**17**	**18**
Area	16	10	4	17	10	12	7	5	14	3	11	12	2	8	1	12	16	1
Region	31	19	7	33	20	23	14	9	27	5	22	24	4	15	1	23	32	1

To solve this situation, the repair algorithm searches other unoccupied regions to place one of the parts that violate Check 1. This search starts by checking whether conjugate region is available. The aim in this is to protect the original version of the chromosome by not changing its original area. If the conjugate region is not available, we first generate an unoccupied region list that the part can be assigned to. It is made of the regions that do not violate Checks 1 and 2. We then assign the part randomly to one of the regions in the list.

Before and after repair of an autoclave charging floor for the layout in Table 4.7 is given in Table 4.8. In this example, the algorithm firstly controls whether Region 2 is available to assign one of the Parts 15 or 18 randomly. As seen, Region 2 is available, and Part 15 can be assigned there. After relocating Part 15, we continue checking regions and detect that Area 12 is over-occupied due to Parts 6 and 16. This time, Region 24 is not available and 4^{th} row is already full. So, one of the parts can be sent to only one the regions from {3, 6, 10, 12, 13, 16, 17, 18, 21, 25, 26, 28, 29, 30, 34, 35, 36}. We then locate Part 16 to Region 30 and all duplication problems are resolved.

Table 4.8 Before and After Repair for Check 1

Before Repair for Check 1								
Area	**Regions**	**Part/s**	**Area**	**Regions**	**Part/s**	**Area**	**Regions**	**Part/s**
1	1, 2	15,18	7	13, 14	7	13	25, 26	
2	3, 4	13	8	15, 16	14	14	27,28	9
3	5, 6	10	9	17, 18		15	29, 30	
4	7, 8	3	10	19, 20	2, 5	16	31, 32	1,17
5	9, 10	8	11	21, 22	11	17	33, 34	4
6	11, 12		12	23, 24	6, 16, 12	18	35, 36	
After Repair for Check 1								
Area	Regions	Part/s	Area	Regions	Part/s	Area	Regions	Part/s
1	1, 2	15,18	7	13, 14	7	13	25, 26	
2	3, 4	13	8	15, 16	14	14	27,28	9
3	5, 6	10	9	17, 18		15	29, 30	16
4	7, 8	3	10	19, 20	2, 5	16	31, 32	1,17
5	9, 10	8	11	21, 22	11	17	33, 34	4
6	11, 12		12	23, 24	6, 12	18	35, 36	

After that, the checking algorithm continues with Check 2. As seen, 4th row has 5 parts violating constraint (6). Again, available regions are detected by eliminating the rows already full. Then, one of the parts is randomly selected and sent to an available region. In this example, Part 5 is chosen and located at Region 18. Table 4.9 shows the final layout of the example above. After these steps, the algorithm continues by controlling Check 3 and Check 4 with the same logic of Check 2.

Table 4.9 After Repair for Check 2 for an Autoclave Charging Floor Layout

After Repair for Check 2								
Area	Regions	Part/s	Area	Regions	Part/s	Area	Regions	Part/s
1	1, 2	15,18	7	13, 14	7	13	25, 26	
2	3, 4	13	8	15, 16	14	14	27,28	9
3	5, 6	10	9	17, 18	5	15	29, 30	16
4	7, 8	3	10	19, 20	2	16	31, 32	1,17
5	9, 10	8	11	21, 22	11	17	33, 34	4
6	11, 12		12	23, 24	6, 12	18	35, 36	

4.2.1.2.1.3. Crowded Tournament Selection Operator

Two solutions are compared by using this operator while determining the mating pool. There are two possible ways to win the tournament for a solution. Firstly, the one with the better Pareto front is the winner. Secondly, if both of them are sharing the same Pareto front, the one with better crowding distance wins the tournament[20].

4.2.1.2.1.4. Crossover Operator

In this study, uniform crossover with crossover probability ($p_c \in [0; 1]$) is used as a crossover operator. In this method, a random number is generated for each pair. If the number is greater than crossover probability, crossover does not occur, and the two parents are replicated as offspring. Otherwise, a binary vector is created to decide which gene of the two chromosomes will be included in the offspring. If 1 is assigned to a gene, offspring *i* takes the assignment from parent *i* and if it is 0, it takes the assignment from the other parent. Figure 4.7 shows an example of the uniform crossover. In this example, crossover is carried over 0100110101 binary vector.

0	1	2	3	4	5	6	7	8	9		3	1	1	5	4	5	9	7	5	9
3	4	1	5	6	7	9	3	5	6	→	0	4	2	3	6	7	6	3	8	6

Figure 4.7 Uniform Crossover

4.2.1.2.1.5. Mutation Operator

As for mutation operator, swap mutation with mutation probability ($p_m \in [0; 1]$) is used. Two genes of a chromosome are chosen randomly, and two values are interchanged if the random number produced for that chromosome is lower than the mutation probability. Otherwise, mutation does not occur. Figure 4.8 shows an example of the swap mutation.

0	1	2	3	4	5	6	7	8	9	→	0	1	2	6	4	5	3	7	8	9

Figure 4.8 Swap Mutation

4.2.1.2.1.6. Fitness Evaluation

We predict the two objective values using regression equations. Knowing the part-region assignments, we find the time to reach the curing temperature for each part. We set the maximum duration as heat-up duration and the difference between maximum and minimum duration as delay.

4.2.1.2.1.7. Improvement Strategy

After obtaining a set of solutions in each generation, we check if we can further improve the objective function values of the solutions in Front 1 by relocating some of the parts. The part that is determinant in both of the objectives is the part that reaches the curing temperature the latest. If this part is placed to another empty region that makes it reach the curing temperature earlier, both of the objective function values improve. Another part that is important in finding the delay is the part that reaches the curing temperature the earliest. If it is also placed to another region that makes it reach the curing temperature later, we may reduce the delay objective.

We start with the part that reaches the curing temperature the latest. Due to having 36 regions and 18 products, there are 18 empty locations that this part can be put. Keeping the feasibility, this part is placed to an unoccupied region and the changes in the two fitness function values are calculated. If the newly obtained solution dominates the previous solution or cannot be dominated by the previous solution, this new solution is added to the population. After all front 1 solutions are evaluated and new solutions generated, sorting is applied again, and fronts are regenerated. Same approach can be also applied to the part that reaches the curing temperature the earliest.

4.2.1.2.1.8. Termination

If prespecified number of generations are achieved, the algorithm stops.

4.2.1.2.2. Implementation of the NSGA-II

Our algorithm consists of the following steps:

Step 0. Initialization

0.1. Create an initial population of size N.

0.2. Perform feasibility check for each solution.

0.3. Feasibility Check

0.3.1. Check the feasibility of all solution in the population.

0.3.2. If the penalty approach is used, increment the fitness values of the infeasible chromosomes.

0.3.3. If the repair approach is used, repair the infeasible chromosomes.

Step 1. Ranking and Parent Selection

1.1. Sort the population into fronts.

1.2. Perform crowded tournament selection to choose the parents.

Step 2. Crossover

2.1. For each pair of parents, generate a random number to decide whether crossover occurs.

2.1.1. If the number generated is larger than the crossover probability, do not conduct crossover and copy the parents to the offspring population.

2.1.2. If the number generated is smaller than the crossover probability, create N/2 binary vectors, conduct uniform crossover using binary vectors and create 2 offspring from each pair.

Step3. Mutation

3.1. For each offspring, generate a random number to decide whether mutation occurs.

3.1.1. If the number generated is larger than the mutation probability, do not conduct mutation.

3.1.2. If the number generated is smaller than the mutation probability, select two genes and change them.

Step 4. Feasibility Check

4.1. Check the feasibility of the offspring population as in Step2.

Step 5. Combined Population

Create a combined population of size 2N by combining the current population with the offspring population, each of size N.

5.1. Determine the fronts of the combined population.

5.2. Take Front 1 solutions and perform Solution Improvement.

Step 6. Solution Improvement

6.1. For each solution in Front 1, determine a part to relocate.

6.2. Find 18 empty regions and derive at most 18 new solutions by locating this part to these locations.

6.3. Check the feasibility of the new solutions and keep only the feasible ones.

6.4. Check if the new solutions are dominated by the previous solutions. If not, keep those new solutions in the combined population.

6.5. Partition the combined population into fronts.

6.6. Select the best N solutions and transfer them to the next population.

Step 7. Termination

Stop if the prespecified number of generations have been achieved. Otherwise, go to Step 1.

Using the structure above, we determine six alternatives to apply NSGA-II to our problem; two alternatives for the constraint handling approach (penalty or repair) and three alternatives for the improvement step (no improvement, relocate t_{lag}, or relocate t_{lead}). These alternatives are given below:

Alternative 1: NSGA-II with repair and no improvement (R/-)

Alternative 2: NSGA-II with penalty and no improvement (P/-)

Alternative 3: NSGA-II with repair and improvement via relocating t_{lag} (R/t_{lag})

Alternative 4: NSGA-II with penalty and improvement via relocating t_{lag} (P/t_{lag})

Alternative 5: NSGA-II with repair and improvement via relocating t_{lead} (R/t_{lead})

Alternative 6: NSGA-II with penalty and improvement via relocating t_{lead} (P/t_{lead})

4.2.1.2.3. Performance Evaluation Metric

Numerous performance metrics have been proposed in the literature[18][21][22] [23][24] to measure the performance of the MOEA[25]. In this paper, we choose to use the hyper-volume indicator. In Figure 4.9, for a bi-objective problem, each nondominated point dominates an area that is shown with rectangles up until a reference point (called as the Nadir point). The hyper-volume of the solution set is the area of the union of all rectangles. In the figure, NSGA-II and ε -constraint method's final nondominated points are shown by circles and squares, respectively. Hyper-volume ratio is calculated by finding the ratio of the area covered by Front 1 solutions of NSGA-II to the area covered by the solutions of the ε -constraint method. The larger the hyper-volume ratio, the better the algorithm[26]. In this study, Nadir Point is set as (1.001, 1.001), and objective function values of all solutions are standardized between 0 and 1 using the minimum and maximum values of all solutions' objective function values.

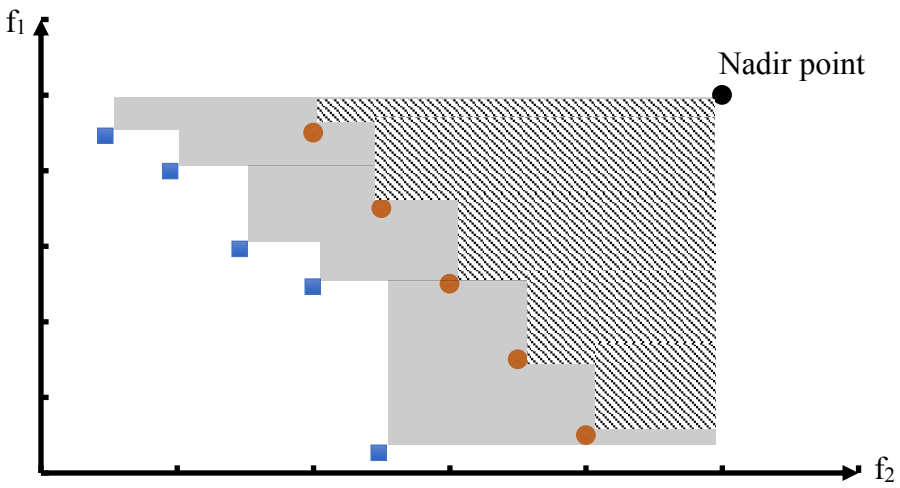

Figure 4.9 Graphical Illustration of the Hyper-volume (HV) Metric

5. COMPUTATIONAL TESTS AND RESULTS

We performed all the computational work by using a computer with Intel Core i7-6700K CPU and 8 GB RAM. CPLEX solver in GAMS software is used to solve *Model L* using the ε -constraint method, and NSGA-II is implemented in MATLAB R2018a. We perform the computational tests in two steps. In the first step, we evaluate the regression models' performance in estimating the times to reach the curing temperature. In the second step, we compare the two solution approaches, generating the nondominated frontier using ε -constraint method and approximating the nondominated frontier using NSGA-II in terms of solution quality and computational times.

5.1. Evaluation of the Regression Models

In this step, we select a previously-loaded group of parts consisting of 18 parts; 6 parts from Family-A, 10 parts from Family-B, 2 parts from Family-C from the past data. According to the data, the heat-up phase lasted for 131 minutes, and the delta between lagging and leading parts was around 41 minutes for the layout used. Using the same set of parts, we find all efficient solutions using the ε-constraint method. We start with a large value for ε, and each time we solve the mathematical model, we set ε to a value that is 0.01 smaller than the last solution's second objective value. These efficient solutions are presented in Table 5.1. The run time to generate all efficient solutions is 13210 CPU seconds. The solutions were evaluated by production engineers and layout of the 5th efficient solution given in Figure 5.1 was chosen to be implemented. Table 5.2 shows the time estimations of the regression models and the observed times of the implementation to reach the curing temperature for 18 parts. According to this layout, our expectation is to reduce it to around 12 minutes. Likewise, our expectation was to reduce the heat-up phase to around 123 minutes. The realizations are indeed close to our estimations. We observe a heat-up period of 125 minutes and a delta value around 19 minutes. The durations to reach the curing temperature for individual parts deviate as much as 10 minutes, where most of the estimations are within 5 minutes of the observed values. This is expected since there may be additional factors that affect the heating transfer between the parts, and regression models are not exact.

In addition to that, while the total process duration of the previously-loaded group was 402 minutes, it decreases to 375 minutes with our layout suggestion. So, there is 27 minutes of gain. Considering that the dwell period is fixed as 120 minutes, we can say

that this gain is achieved by 6 minutes shortening in heat-up and 21 minutes shortening in cooling duration. Although we did not make an analysis for the cooling phase, it was naturally affected by the initial placement in the autoclave.

Table 5.1 GAMS Results

Efficient Solution	**1**	**2**	**3**	**4**	**5**	**6**
t_{lag} (min)	115.28	120.46	120.92	121.19	122.95	130.55
Delta (min)	23.19	22.99	21.10	17.99	12.19	11.42

Area 1 Part 14 | Part 17	**Area 7** Part 7 | Part 11	**Area 13**
Area 2 Part 1 | Part 5	**Area 8** Part 8 | Part 10	**Area 14**
Area 3	**Area 9**	**Area 15** Part 13 | Part18
Area 4 Part 2 | Part 16	**Area 10**	**Area 16** Part 6 | Part 9
Area 5 Part 3 | Part 4	**Area 11**	**Area 17**
Area 6	**Area 12**	**Area 18** Part 12 | Part 15

Figure 5.1 Layout of Efficient Solution 5

Table 5.2 Predicted vs. Realized Times to Reach Curing Temperature (min)

	Predicted T (min)	**Realized T (min)**	**Difference (min)**
Part 1	122.95	117.93	5.02
Part 2	122.07	120.98	1.09
Part 3	115.28	111.83	3.50
Part 4	115.41	118.95	-3.54
Part 5	122.95	125.05	-2.10
Part 6	120.62	110.82	9.80
Part 7	112.84	106.75	6.09
Part 8	121.44	120.98	0.46
Part 9	121.72	113.87	7.85
Part 10	121.95	114.88	7.07
Part 11	112.84	108.78	4.06
Part 12	110.78	105.73	5.05
Part 13	114.81	105.73	9.08
Part 14	112.78	106.75	6.03
Part 15	110.78	112.85	-2.07
Part 16	114.03	114.88	-0.86
Part 17	121.06	123.02	-1.99
Part 18	112.44	117.93	-5.49
t_{lag}	122.95	125.05	-2.10
t_{lead}	110.78	105.73	5.05
Delta	12.18	19.32	-7.14

5.2. Determining the Mechanisms for NSGA-II

We next find the best alternative for NSGA-II. For this, we evaluate the results of all alternatives in terms of closeness to the exact solutions via HVI (Hyper-volume Indicator). In addition to HVI, computational time is also a concern due to practical use of the algorithm. To begin with, we chose a batch including 18 parts and found the efficient layouts of it using the ε -constraint method. We employ ε -constraint method as explained in Section 5.1. We found 13 efficient solutions. Then, we run all six alternative implementations of NSGA-II five times for this batch.

Depending on the similar experiments in the literature[10][27][28][29][30][31], both the population size (N) and the number of generations are set to 100. As for crossover probability (p_c) and mutation probability (p_m), they were decided as 0.8 and 0.6, respectively. The average HVI's and computational times of the five runs are given in Table 5.3. As seen in the table, all computational times are quite shorter than the computational time of the ε-constraint method. The repair mechanism always performs better than the penalty approach in terms of HVI measure in exchange for a slight increase in the computational times. Relocating the lagging part also proves to be efficient according to the results. As a result, relocating the lagging part and employing the repair mechanism seems to be the best alternative with HVI value of 0.84. We continue with these mechanisms in our further computations.

Table 5.3 HVI and CPU Results of Six Different Alternatives for NSGA-II

	HVI	**CPU (s)**
Alternative 1 (R/-)	0.70	30.19
Alternative 2 (P/-)	0.17	25.08
Alternative 3 (R/t_{lag})	0.84	47.88
Alternative 4 (P/t_{lag})	0.76	47.05
Alternative 5 (R/t_{lead})	0.48	49.09
Alternative 6 (P/t_{lead})	0.36	47.39

As a second step, we run NSGA-II for different values of parameters N, p_c, p_m using same batch. We use two values for N (100 and 200), three values for p_c (0.4, 0.6, and 0.8), and two values for p_m (0.8 and 0.9), and run each combination five times with different seeds. The average HVI values and run times of five trials for all settings are given in Table 5.4. The HVI values are large enough for both population sizes. However, considering the run times, population size of 200 runs approximately 4 times longer than the population size of 100. There is a difference of about 2 minutes between the two populations. This

difference becomes significant when it is assumed that at the beginning of the week about 21 plans will be made at the same time. But if daily planning is to be made, N = 200 can be also used. In this study, we prefer to continue with the population size of 100. As seen from the table, run times are very close for this population size for all p_m and p_c values. Thus, run times are not a decisive factor this time and we can choose p_m and p_c values only by looking at the HVI values. Consequently, with the HVI value of 0.84, the p_c, p_m are both set to 0.8.

Table 5.4 HVI and CPU Results of Algorithm 3

	p_c	p_m	HVI	CPU (s)
N=100	0.4	0.8	0.75	45.22
	0.6		0.69	47.78
	0.8		0.84	47.88
	0.4	0.9	0.77	46.08
	0.6		0.78	47.18
	0.8		0.83	48.68
N=200	0.4	0.8	0.82	165.02
	0.6		0.84	170.73
	0.8		0.86	174.07
	0.4	0.9	0.79	166.88
	0.6		0.80	170.88
	0.8		0.85	173.89

5.3. Evaluation of NSGA-II

After deciding on the setting of NSGA-II, we compare NSGA-II with the ε −constraint method using five different batches. We use the batches explained in Sections 5.1 and 5.2 as Batch 1 and Batch 2, and choose three additional batches from the previous data. All batches contain 18 parts and differ from each other in content and layout. We first generate each batch's efficient solutions using the ε-constraint method. We then approximate the efficient solutions using NSGA-II with the setting chosen in the previous sections. The number of efficient solutions of all batches are reported in the first column of Table 5.5, and the results of the two methods are given in columns 2-4. The HVI value of Batch 2 and Batch 5 are lower than the others due to having fewer efficient solutions. For the remaining three batches, the HVI values are greater than 0.75. The solution times of NSGA-II are considerably smaller than the duration of the ε −constraint method.

We also give the spread of the real efficient set and the approximated set in Figures 5.2-5.6 for all batches. We choose one of the five runs to show the effectiveness of the NSGA-

II. The spread of NSGA-II is close to the efficient set, especially if the number of efficient solutions is larger. NSGA-II approximates the middle solutions better, and in general misses the extreme solutions. This is acceptable, since for implementation, middle solutions are preferred. Also, we found the distance of each solution of NSGA-II to the nearest efficient solution by using Chebyshev distance metric and calculated their average for each run. The average distance for all runs is less than 4.2, with a range from 0.3 to 6.8. So, the delay and the heat-up phase of any solution of NSGA-II is, on the average, at most 4.2 minutes more than those of the closest efficient solution. This is a reasonable deviation considering the factory activities. Overall, the performance of NSGA-II in terms of both computational times and closeness to real efficient solutions is satisfactory. If the planner needs to decide on a layout for a batch in short times, the efficient set can be approximated using NSGA-II initially. A layout can be chosen to be implemented, or efficient solutions close to that layout can be searched with bounds set on the two-objective function.

Table 5.5 Results for 5 Different Batches

	Number of Efficient Solutions	**ε -constraint method**	**NSGA-II**	
		CPU (s)	**HVI**	**CPU (s)**
Batch 1	13	13320	0.83	49.70
Batch 2	6	13210	0.51	54.09
Batch 3	12	11189	0.91	49.90
Batch 4	10	5587	0.77	55.85
Batch 5	5	1924	0.44	54.32

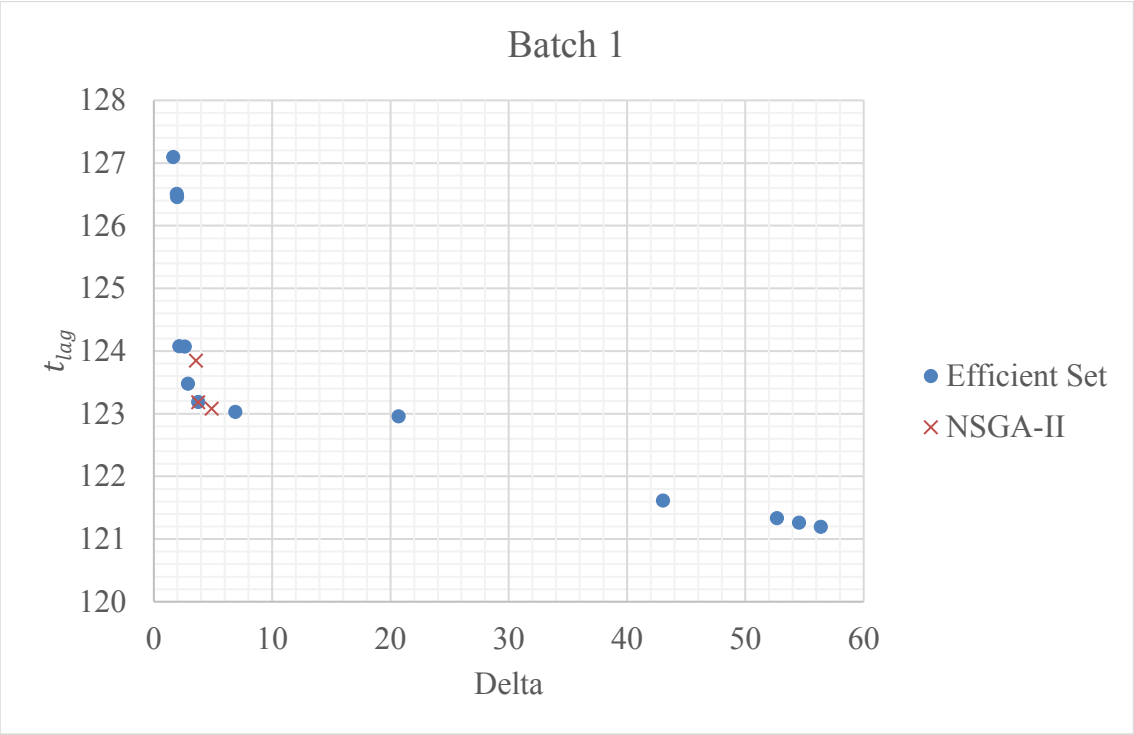

Figure 5.2 Results of Both Methods for Batch 1

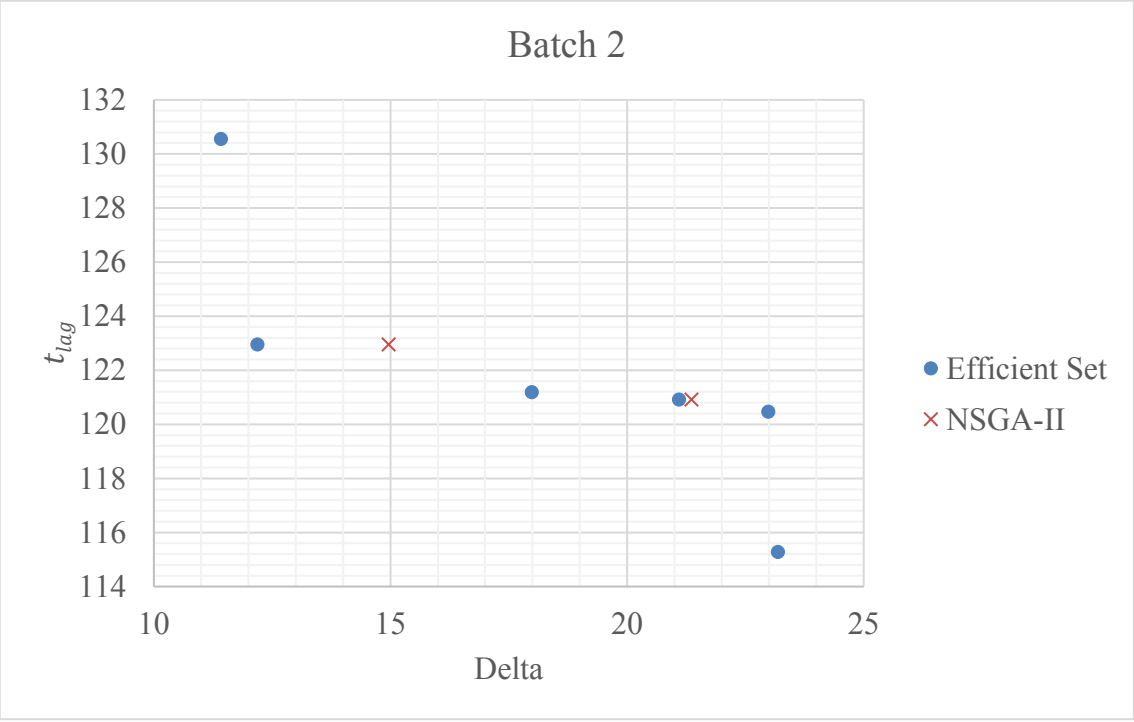

Figure 5.3 Results of Both Methods for Batch 2

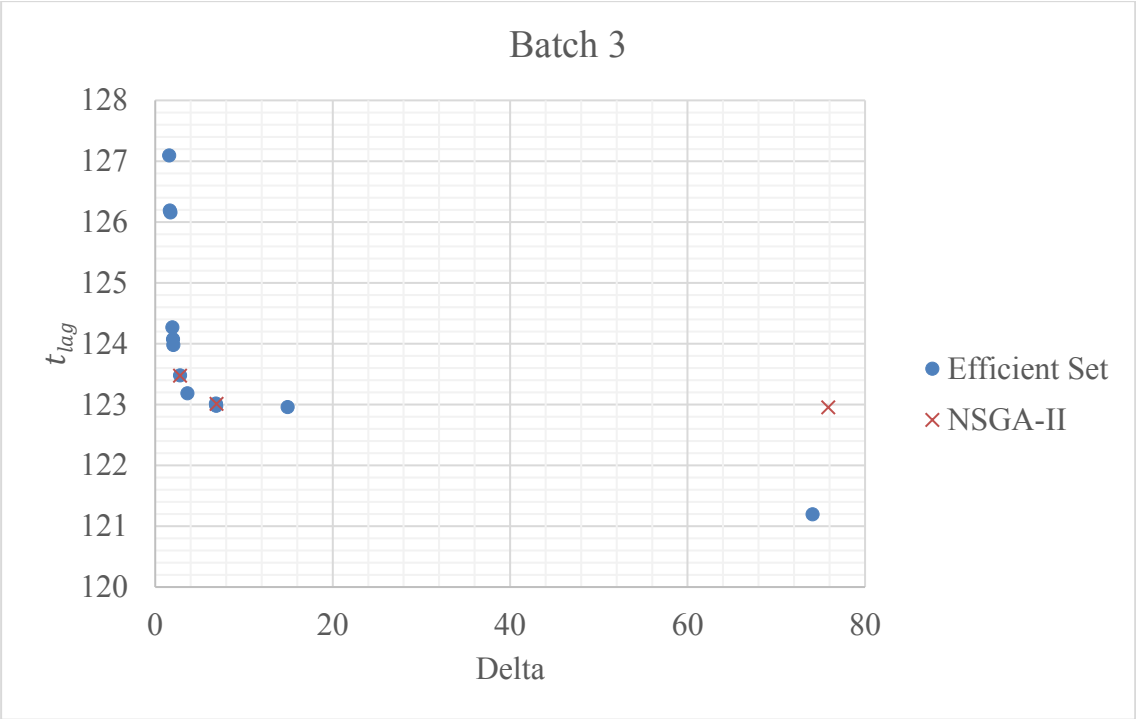

Figure 5.4 Results of Both Methods for Batch 3

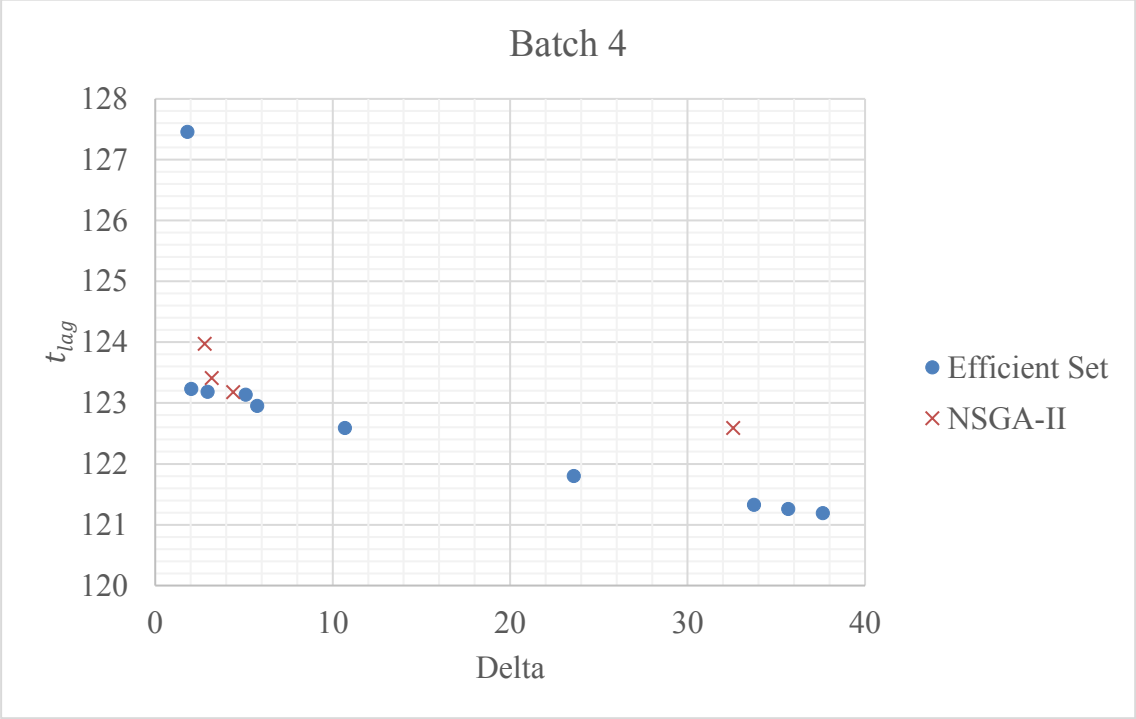

Figure 5.5 Results of Both Methods for Batch 4

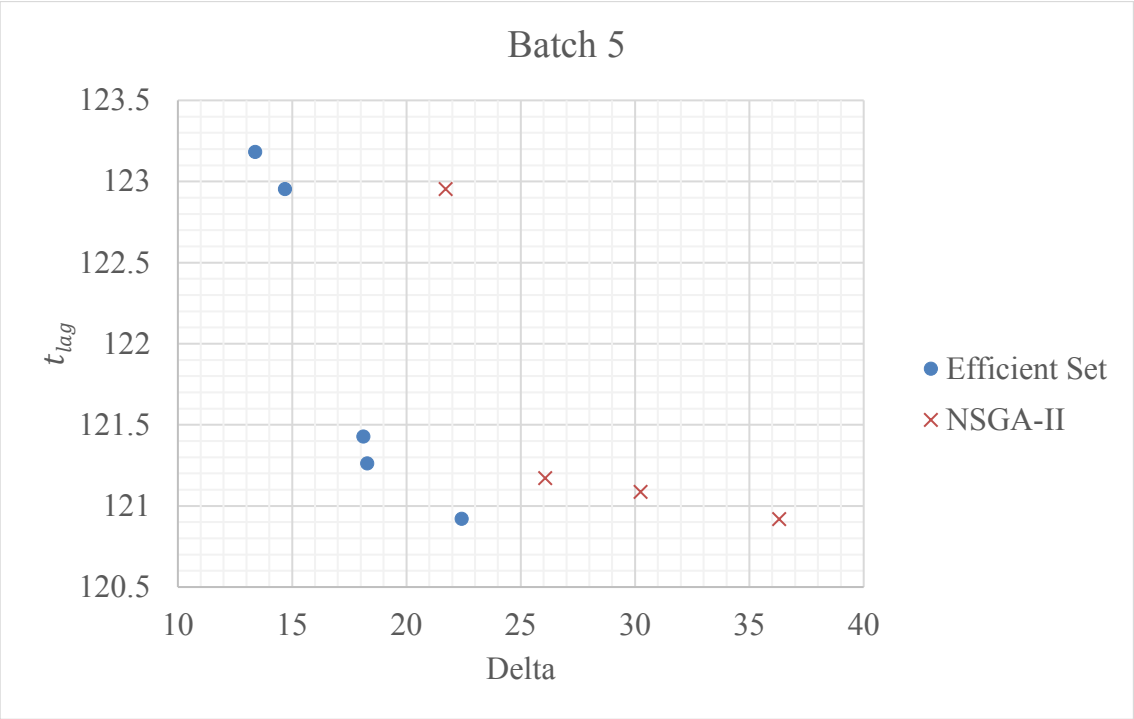

Figure 5.6 Results of Both Methods for Batch 5

6. CONCLUSIONS AND FUTURE WORK

The autoclave curing cycle that is made of three phases: heat-up phase, dwell period, and cooling phase. We consider the heat-up phase of this cycle and develop approaches to place parts in the autoclave while minimizing the duration of the heat-up phase and minimizing the delay between parts in reaching the curing temperature. We employ a two-stage approach. In the first stage, we use multiple regression to estimate the time to reach the curing temperature. With this aim, firstly, autoclave data collected in the recent years was investigated to determine the factors affecting the time to reach the curing temperature. The most important factors are decided as the location, total batch weight, individual part weight, length and width of the part, and weight of the parts in front of each part until the door. We then divide the autoclave into 18 areas and obtain regression models for each area which enables to predict the time to reach the curing temperature when a part is placed on that specific area. All predictor variables and their combinations are included in the regression model and the significant ones are selected with stepwise regression. We obtain different equations for each area with satisfactory estimation power.

In the second stage, we determine the efficient placements of parts in the autoclave. Our initial mathematical model is a MINLPM which we then convert into an equivalent MILPM. We then generate the whole efficient solutions by the ε -constraint method. One of the efficient solutions of a batch is implemented in the autoclave. As well as proving that our estimations were very close to realizations, it resulted in a significant reduction in the heat-up phase. We also develop mechanisms for NSGA-II to solve the parts placement problem optimizing the two objectives explained above. Specifically, we develop a repair mechanism to repair infeasible solutions that violate at least one of the four constraints. We also propose an improvement mechanism that allows obtaining new efficient solutions when the part that reaches the curing temperature the latest is replaced to one of the empty regions in a layout. The demonstrations on five different batches show that NSGA-II approximates the efficient solutions well. The average hypervolume indicator is 0.70 and NSGA-II runs in significantly shorter duration when compared with the solution times of the exact method. This algorithm can be used as an alternative to the exact method when solutions are needed in short times in cases such as a change in the batch composition.

By the proposed solution methods in this study, it will be possible to predict the time to reach the curing temperature for a batch of parts, and to develop a layout that minimizes the heat-up period and the time delay between reaching the curing temperature. As a result of this study, as well as facilitating production engineer's work in deciding how to place a batch during autoclave loading, the composite parts will be produced in standard quality, in a shorter period and with less cost.

As a future study, more predictor variables can be used while developing regression models. In addition to that, in spite of the fact that the proposed technique was applied to a particular autoclave, the procedure can be generalized for different types of parts and autoclaves with different sizes. We currently find the best placement of a set of parts in the autoclave. If we have more parts than the capacity of the autoclave to be loaded, the grouping of parts to batches is another interesting research direction.

REFERENCES

[1] M. Dios, P. L. Gonzalez-R, D. Dios, and A. Maffezzoli, "A mathematical modeling approach to optimize composite parts placement in autoclave," *International Transactions in Opereational. Research*, vol. 24, no. 1–2, pp. 115–141, **2017.**

[2] E. Eryıldız and A. Akdoğan Eker, "Savunma Sanayinde Kullanılan İleri Kompozit Malzemeler ve Uygulama Alanları," *International Journal of Engineering Research and Development, Vol.7, No.4,* **2015.**

[3] L. Wang, W. Zhu, Q. Wang, Q. Xu, and Y. Ke, "A heat-balance method for autoclave process of composite manufacturing," *Journal of Composite Materials*, vol. 53, no. 5, pp. 641–652, **2019.**

[4] Q. Wang, L. Wang, W. Zhu, Q. Xu, and Y. Ke, "Numerical investigation of the effect of thermal gradients on curing performance of autoclaved laminates," *Journal of Composite Materials*, vol. 54, no. 1, pp. 127–138, **2020.**

[5] J. Hu, L. Zhan, X. Yang, R. Shen, J. He, and N. Peng, "Temperature optimization of mold for autoclave process of large composite manufacturing," *Journal of Physics: Conference Series.*, vol. 1549, no. 3, **2020.**

[6] V. Haskilic, "Kompozit Üretiminde Otoklav Yükleme Ve Çizelgeleme İçin Yeni Bir Model Önerisi : Savunma Sanayii Uygulaması," **2019.**

[7] A. Maffezzoli and A. Grieco, "Optimization of parts placement in autoclave processing of composites," *Applied Composite Materials*, vol. 20, no. 3, pp. 233–248, **2013.**

[8] C. S. Chen, S. M. Lee, and Q. S. Shen, "An analytical model for the container loading problem," *European Journal of Operational Research*, vol. 80, no. 1, pp. 68–76, **1995.**

[9] L. Nele, A. Caggiano, and R. Teti, "Autoclave Cycle Optimization for High Performance Composite Parts Manufacturing," *Procedia CIRP*, vol. 57, pp. 241–246, **2016.**

[10] M. G. Misola and B. B. Navarro, "Optimal facility layout problem solution using generic algorithm," *International Journal of Mechanical, Aerospace, Industrial, Mechatronic and Manufacturing Engineering*, vol. 7, no. 8, pp. 1691–1696, **2013.**

[11] H. Hosseini-Nasab, S. Fereidouni, S. M. T. Fatemi Ghomi, and M. B. Fakhrzad, "Classification of facility layout problems: a review study," *The International Journal of Advanced Manufacturing Technology*, vol. 94, no. 1–4, pp. 957–977, **2018.**

[12] M. Köksalan and D. Tezcaner Öztürk, "An evolutionary approach to generalized biobjective traveling salesperson problem," *Computers&OperationsResearch*, vol. 79, pp. 304–313, **2017.**

[13] A. Michael Olusegun, "Identifying the Limitation of Stepwise Selection for Variable Selection in Regression Analysis," *American Journal of Theoretical and Applied Statistics*, vol. 4, no. 5, p. 414, **2015.**

[14] J. O. Rawlings, S. G. Pantula, D. A. Dickey, *Applied Regression Analysis: A Research Tool, 2nd ed.*, Springer-Verlag New York, **2018.**

[15] A. Field, *Discovering Statistics Using IBM SPSS Statistics: And Sex and Drugs and Rock 'n' Roll,* 3rd ed., SAGE Publications Ltd., London, **2009.**

[16] S. A. Lesik, *Applied statistical inference with MINITAB®*, CRC Press Taylor & Francis Group, LLC, Florida, **2009.**

[17] J. Puchinger and G. R. Raidl, "Combining metaheuristics and exact algorithms in combinatorial optimization: A survey and classification," *International Work-Conference on the Interplay Between Natural and Artificial Computation*, pp. 41-53, **2005.**

[18] D. A. Van Veldhuizen and G. B. Lamont, "Multiobjective evolutionary algorithms: analyzing the state-of-the-art.," *Evolutionary computation*, **2000.**

[19] K. Deb, A. Pratap, S. Agarwal, and T. Meyarivan, "A fast and elitist multiobjective genetic algorithm: NSGA-II," *IEEE Transactıons on Evolutıonary Computatıon*, vol. 6, no. 2, pp. 182–197, **2002.**

[20] K. Deb, "Multi-objective Optimisation Using Evolutionary Algorithms: An Introduction," in *Multi-objective Evolutionary Optimisation for Product Design and Manufacturing*, **2011.**

[21] D. Knowles, J. and Corne, "On metrics for comparing nondominated sets," *Evolutionary Computation,* vol. 1, pp. 711–716, **2002.**

[22] E. Zitzler, L. Thiele, M. Laumanns, C. M. Fonseca, and V. G. Da Fonseca, "Performance assessment of multiobjective optimizers: An analysis and review," *IEEE Transactions on Evolutionary Computation*, **2003.**

[23] E. Zitzler, K. Deb, and L. Thiele, "Comparison of multiobjective evolutionary algorithms: empirical results.," *Evolutionary Computation*, **2000.**

[24] A. Zhou, B. Y. Qu, H. Li, S. Z. Zhao, P. N. Suganthan, and Q. Zhangd, "Multiobjective evolutionary algorithms: A survey of the state of the art," *Swarm and Evolutionary Computation*, **2011.**

[25] K. T. Lwin, R. Qu, and B. L. MacCarthy, "Mean-VaR portfolio optimization: A nonparametric approach," *European Journal of Operational Research,* **2017.**

[26] Y. Li, F. Chu, C. Feng, C. Chu, and M. C. Zhou, "Integrated Production Inventory Routing Planning for Intelligent Food Logistics Systems," *IEEE Intelligent Transportation Systems Transactions*, vol. 20, no. 3, pp. 867–878, **2019.**

[27] S. Yamani Douzi Sorkhabi, D. A. Romero, J. C. Beck, and C. H. Amon, "Constrained multi-objective wind farm layout optimization: Novel constraint handling approach based on constraint programming," *Renewable Energy*, **2018.**

[28] F. Azadivar and J. Wang, "Facility layout optimization using simulation and genetic algorithms," *International Journal of Production Research*, **2000.**

[29] N. Srinivas and K. Deb, "Muiltiobjective Optimization Using Nondominated Sorting in Genetic Algorithms," *Evolutionary Computation*, **1994.**

[30] A. Ghosh and M. K. Das, "Non-dominated rank based sorting genetic algorithms," *Fundamenta Informaticae*, **2008.**

[31] O. Abdoun, J. Abouchabaka, and C. Tajani, “Analyzing the Performance of Mutation Operators to Solve the Travelling Salesman Problem,” **2012.**

APPENDIX A

AREA 1:

Number of data: 11

Analysis of Variance

Source	DF	Adj SS	Adj MS	F-Value	P-Value
Regression	3	2224,1	741,36	32,10	0,000
B	1	118,7	118,74	5,14	0,058
P	1	1271,1	1271,09	55,03	0,000
L*L	1	327,9	327,91	14,20	0,007
Error	7	161,7	23,10		
Total	10	2385,8			

Model Summary

S	R-sq	R-sq(adj)	R-sq(pred)
4,80585	93,22%	90,32%	84,04%

Coded Coefficients

Term	Coef	SE Coef	T-Value	P-Value	VIF
Constant	99,39	2,82	35,23	0,000	
B	0,01690	0,00745	2,27	0,058	2,42
P	-0,1872	0,0252	-7,42	0,000	1,96
L*L	0,02008	0,00533	3,77	0,007	1,34

Regression Equation in Coded Units

MaxTime = 99,39 + 0,01690 B - 0,1872 P + 0,02008 L*L

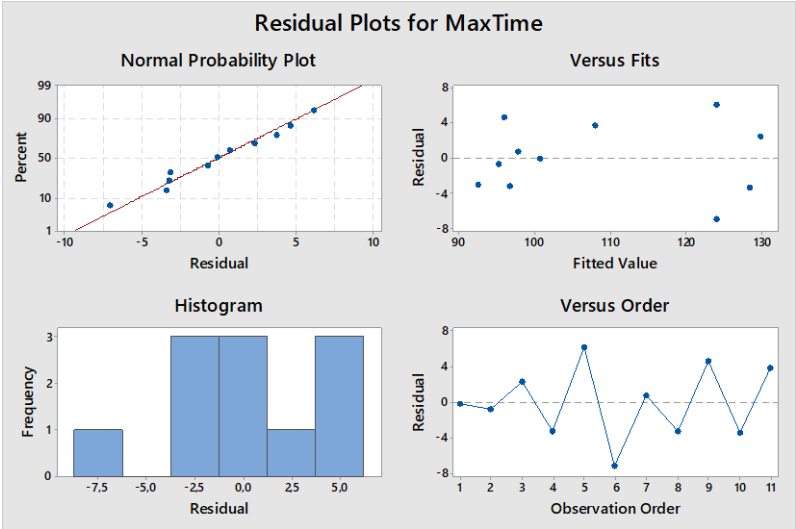

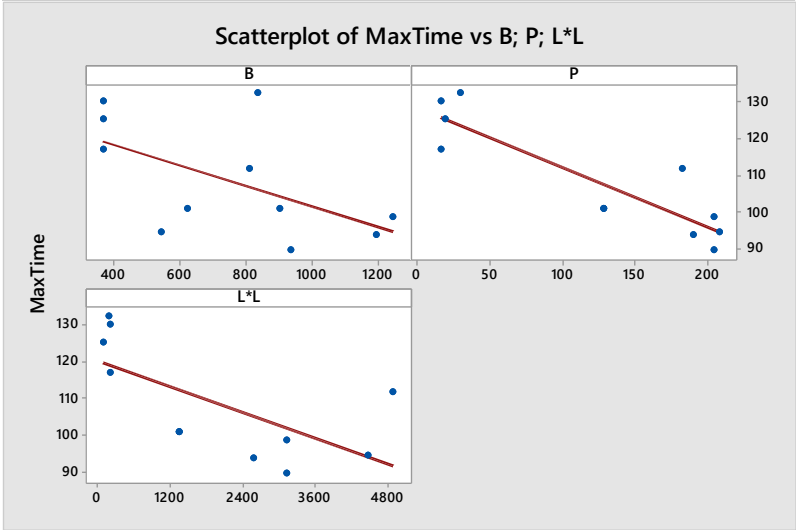

AREA 2:

Number of data: 31

Analysis of Variance

Source	DF	Adj SS	Adj MS	F-Value	P-Value
Regression	3	6021	2006,96	46,00	0,000
L	1	3339	3338,53	76,52	0,000
P*L	1	2478	2477,87	56,79	0,000
P*W	1	1462	1462,29	33,52	0,000
Error	27	1178	43,63		
Total	30	7199			

Model Summary

S	R-sq	R-sq(adj)	R-sq(pred)
6,60528	83,64%	81,82%	78,78%

Coded Coefficients

Term	Coef	SE Coef	T-Value	P-Value	VIF
Constant	100,41	1,83	55,01	0,000	
L	-0,6400	0,0732	-8,75	0,000	1,27
P*L	0,01165	0,00155	7,54	0,000	2,03
P*W	-0,0624	0,0108	-5,79	0,000	2,34

Regression Equation in Coded Units

MaxTime = 100,41 - 0,6400 L + 0,01165 P*L - 0,0624 P*W

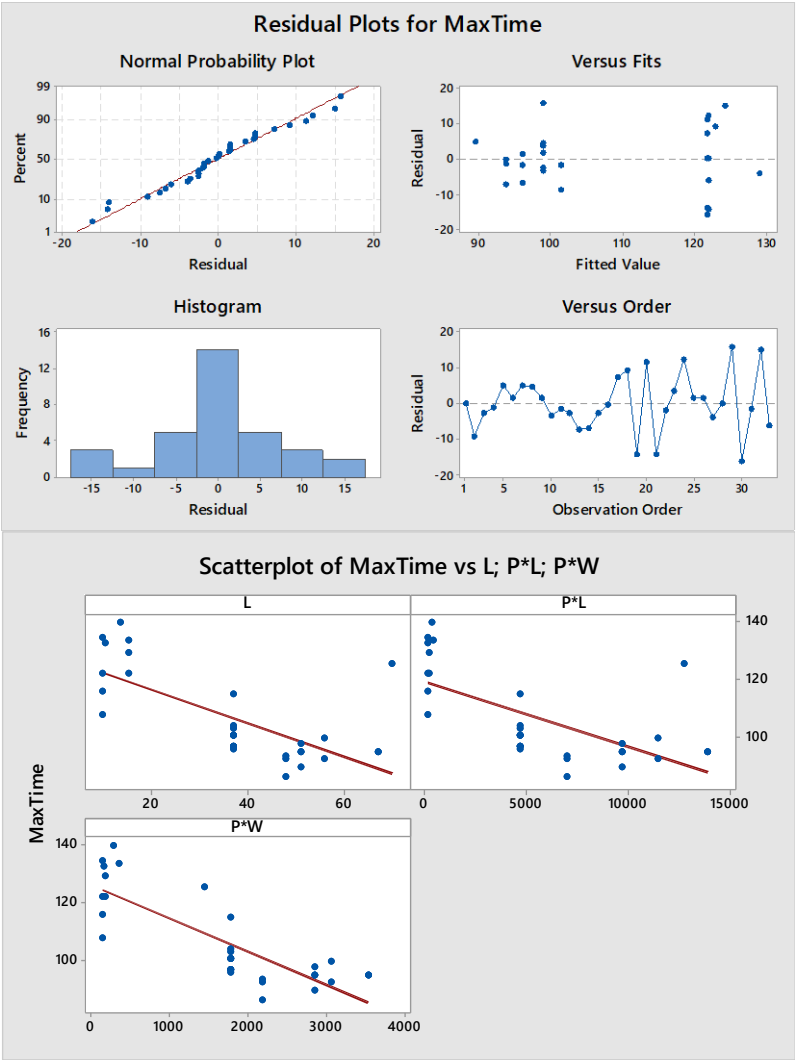

AREA 3:

Number of data: 35

Analysis of Variance

Source	DF	Adj SS	Adj MS	F-Value	P-Value
Regression	3	8638,60	2879,53	91,31	0,000
L	1	7909,28	7909,28	250,79	0,000
B*B	1	91,80	91,80	2,91	0,098
P*L	1	432,09	432,09	13,70	0,001
Error	31	977,64	31,54		
Total	34	9616,25			

Model Summary

S	R-sq	R-sq(adj)	R-sq(pred)
5,61577	89,83%	88,85%	86,24%

Coded Coefficients

Term	Coef	SE Coef	T-Value	P-Value	VIF
Constant	100,51	2,53	39,67	0,000	
L	-0,7131	0,0450	-15,84	0,000	1,02
B*B	0,000014	0,000008	1,71	0,098	1,05
P*L	0,00477	0,00129	3,70	0,001	1,04

Regression Equation in Coded Units

MaxTime = 100,51 - 0,7131 L + 0,000014 B*B + 0,00477 P*L

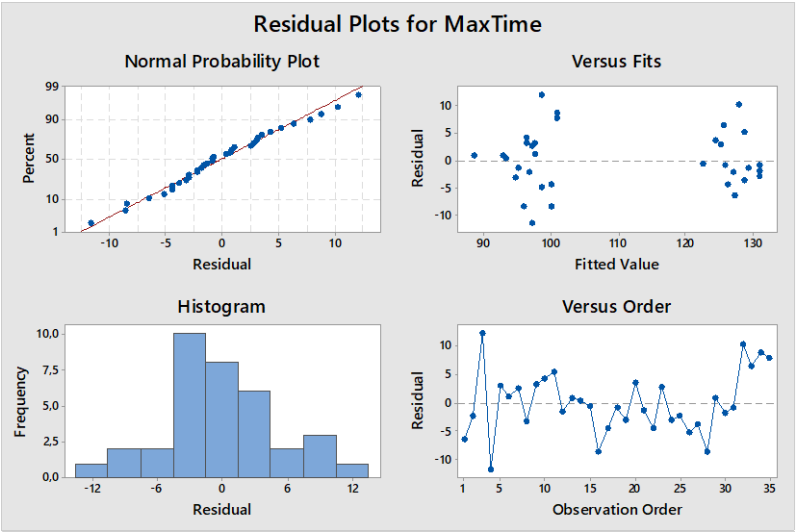

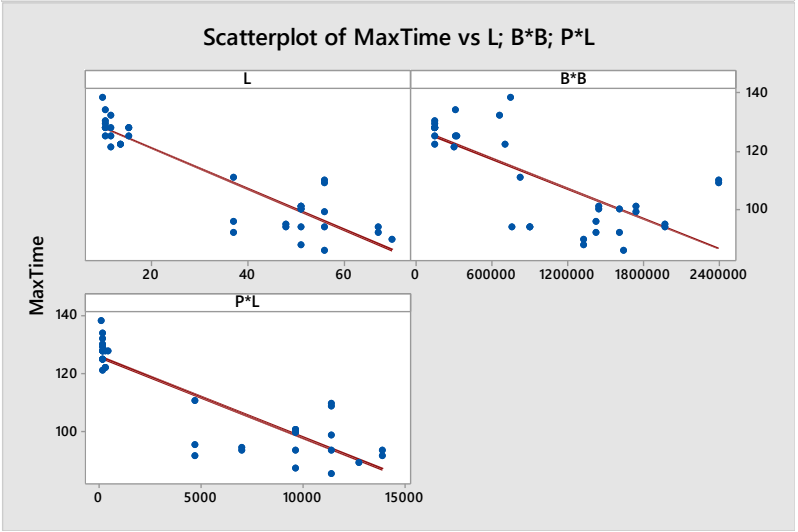

AREA 4:

Number of data: 51

Analysis of Variance

Source	DF	Adj SS	Adj MS	F-Value	P-Value
Regression	3	9383,3	3127,76	78,35	0,000
P	1	971,9	971,89	24,34	0,000
W	1	1118,6	1118,58	28,02	0,000
F*W	1	517,2	517,23	12,96	0,001
Error	47	1876,4	39,92		
Lack-of-Fit	45	1842,9	40,95	2,45	0,333
Pure Error	2	33,5	16,73		
Total	50	11259,7			

Model Summary

S	R-sq	R-sq(adj)	R-sq(pred)
6,31844	83,34%	82,27%	79,20%

Coded Coefficients

Term	Coef	SE Coef	T-Value	P-Value	VIF
Constant	114,911	0,946	121,49	0,000	
P	-0,0902	0,0183	-4,93	0,000	2,53
W	-2,817	0,532	-5,29	0,000	2,51
F*W	-0,01877	0,00521	-3,60	0,001	1,01

Regression Equation in Coded Units

MaxTime = 114,911 - 0,0902 P - 2,817 W - 0,01877 F*W

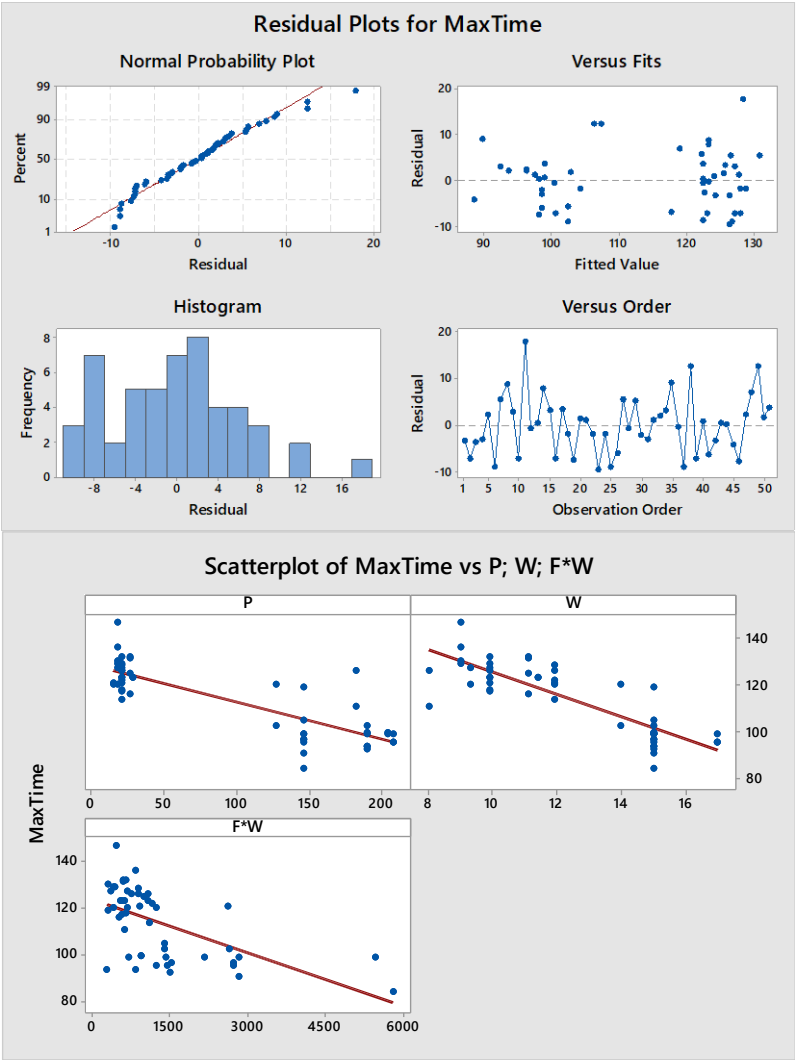

AREA 5:

Number of data: 70

Analysis of Variance

Source	DF	Adj SS	Adj MS	F-Value	P-Value
Regression	4	3174,90	793,73	11,55	0,000
B	1	296,89	296,89	4,32	0,042
F	1	1407,70	1407,70	20,48	0,000
P*W	1	327,81	327,81	4,77	0,033
W*F	1	2834,93	2834,93	41,24	0,000
Error	65	4467,97	68,74		
Lack-of-Fit	63	4455,05	70,72	10,95	0,087
Pure Error	2	12,92	6,46		
Total	69	7642,87			

Model Summary

S	R-sq	R-sq(adj)	R-sq(pred)
8,29084	41,54%	37,94%	30,49%

Coded Coefficients

Term	Coef	SE Coef	T-Value	P-Value	VIF
Constant	129,10	1,05	122,73	0,000	
B	0,00555	0,00267	2,08	0,042	1,02
F	0,2222	0,0491	4,53	0,000	2,46
P*W	0,02006	0,00918	2,18	0,033	1,19
W*F	0,1397	0,0218	6,42	0,000	2,25

Regression Equation in Coded Units

MaxTime = 129,10 + 0,00555 B + 0,2222 F + 0,02006 P*W
+ 0,1397 W*F

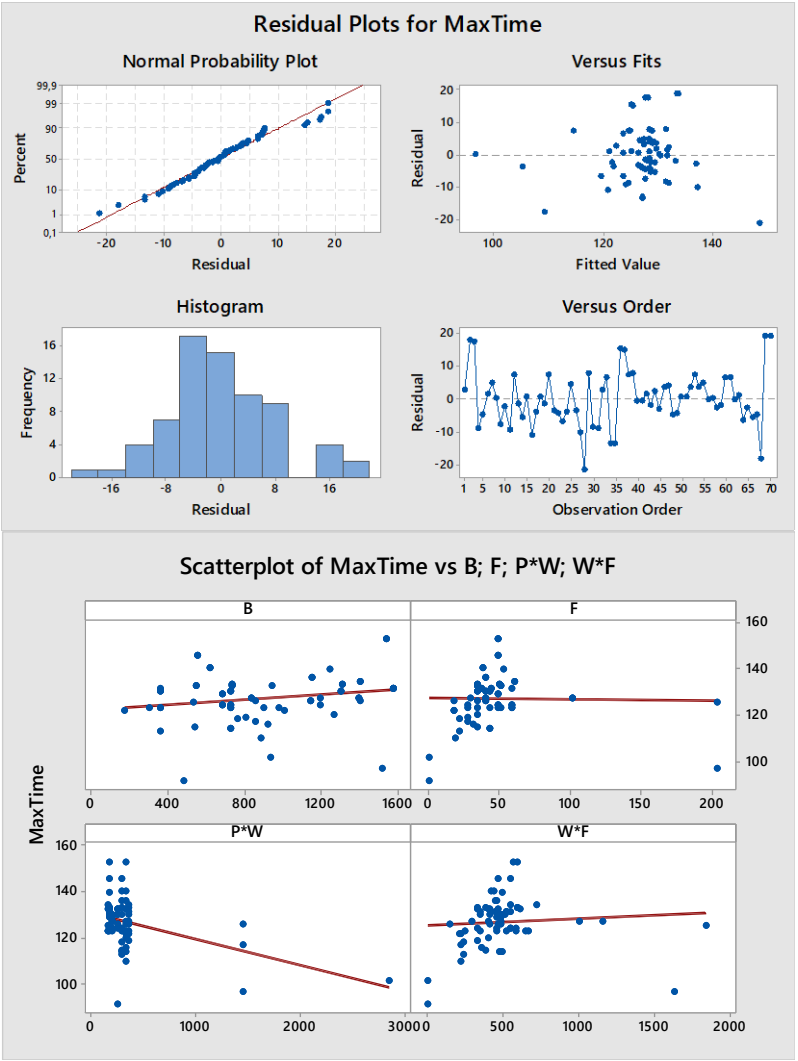

AREA 6:

Number of data: 101

Analysis of Variance

Source	DF	Adj SS	Adj MS	F-Value	P-Value
Regression	1	9215	9214,94	161,97	0,000
P	1	9215	9214,94	161,97	0,000
Error	99	5632	56,89		
Lack-of-Fit	82	4510	55,00	0,83	0,717
Pure Error	17	1123	66,04		
Total	100	14847			

Model Summary

S	R-sq	R-sq(adj)	R-sq(pred)
7,54278	62,06%	61,68%	59,57%

Coded Coefficients

Term	Coef	SE Coef	T-Value	P-Value	VIF
Constant	122,171	0,751	162,78	0,000	
P	-0,1849	0,0145	-12,73	0,000	1,00

Regression Equation in Uncoded Units

MaxTime = 129,688 - 0,1849 P

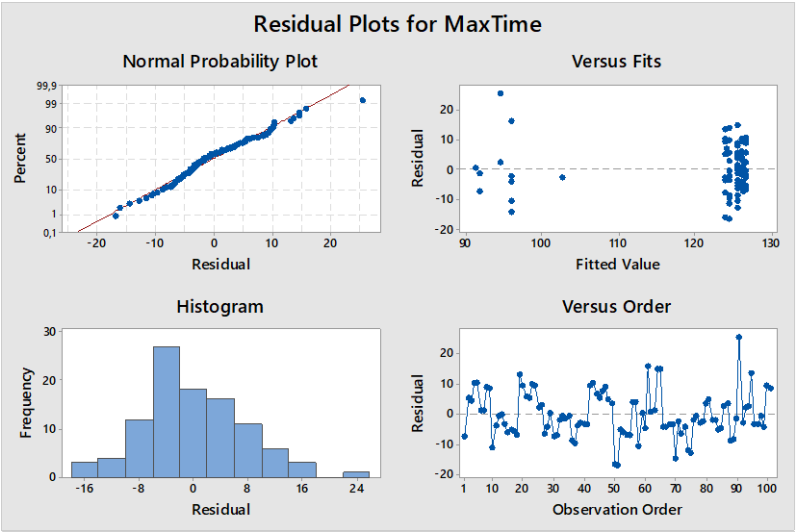

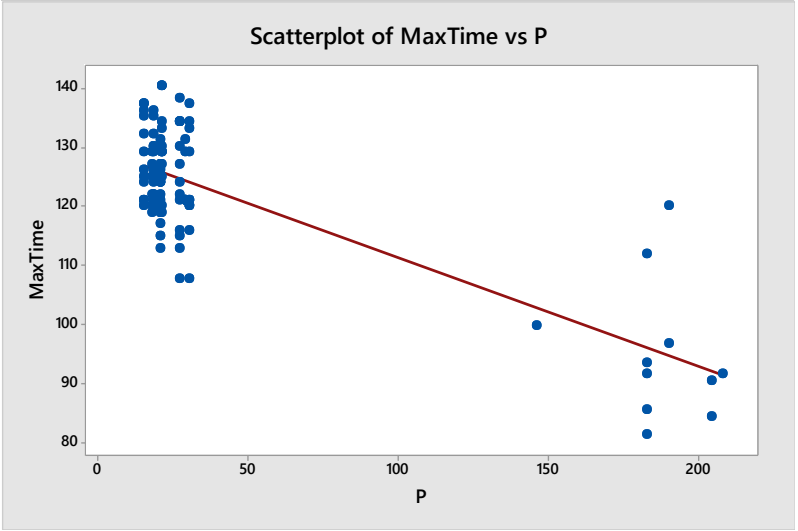

AREA 7:

Number of data: 8

Analysis of Variance

Source	DF	Adj SS	Adj MS	F-Value	P-Value
Regression	3	923,85	307,95	21,21	0,006
B	1	140,15	140,15	9,65	0,036
F	1	134,35	134,35	9,25	0,038
B*F	1	299,97	299,97	20,66	0,010
Error	4	58,08	14,52		
Total	7	981,93			

Model Summary

S	R-sq	R-sq(adj)	R-sq(pred)
3,81050	94,09%	89,65%	77,36%

Coded Coefficients

Term	Coef	SE Coef	T-Value	P-Value	VIF
Constant	99,25	2,59	38,37	0,000	
B	-0,02004	0,00645	-3,11	0,036	2,84
F	-0,0769	0,0253	-3,04	0,038	7,13
B*F	0,000258	0,000057	4,55	0,010	4,06

Regression Equation in Uncoded Units

MaxTime = 168,30 - 0,0671 B - 0,2885 F + 0,000258 B*F

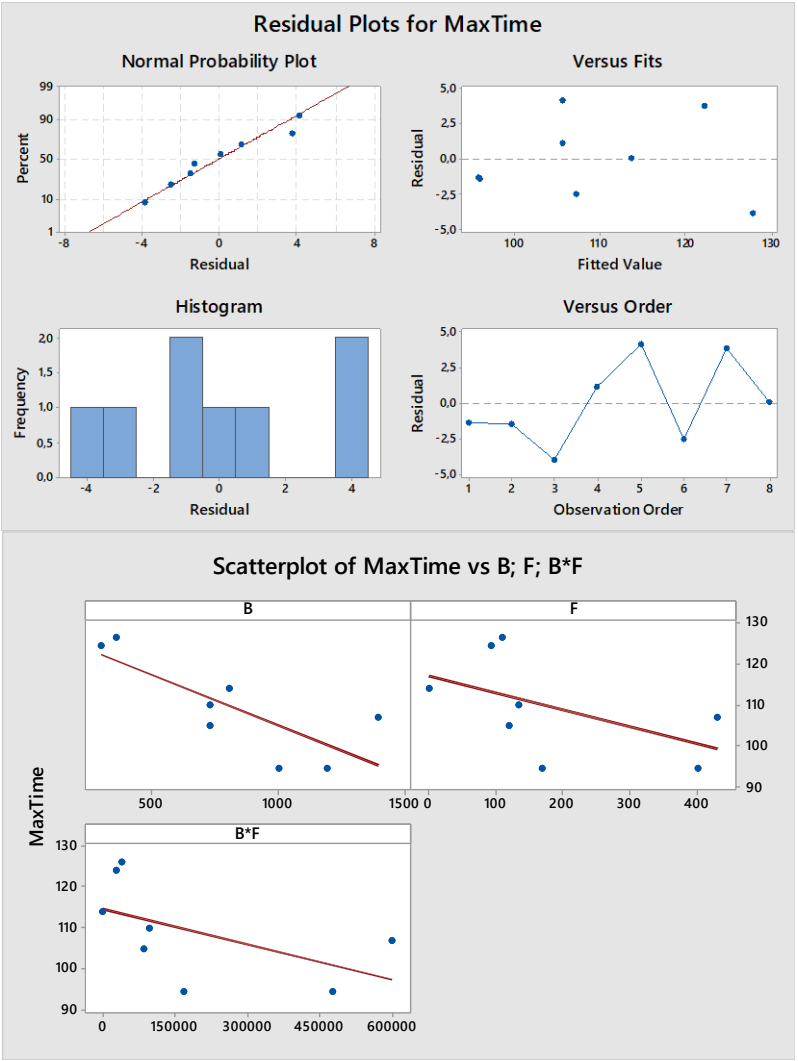

AREA 8:

Number of data: 23

Analysis of Variance

Source	DF	Adj SS	Adj MS	F-Value	P-Value
Regression	3	2746,1	915,37	30,00	0,000
P	1	985,2	985,22	32,29	0,000
P*P	1	641,3	641,32	21,02	0,000
W*L	1	426,1	426,13	13,97	0,001
Error	19	579,7	30,51		
Total	22	3325,8			

Model Summary

S	R-sq	R-sq(adj)	R-sq(pred)
5,52357	82,57%	79,82%	68,96%

Coded Coefficients

Term	Coef	SE Coef	T-Value	P-Value	VIF
Constant	99,28	1,77	56,17	0,000	
P	-0,1352	0,0238	-5,68	0,000	1,65
P*P	0,001592	0,000347	4,58	0,000	1,37
W*L	-0,0800	0,0214	-3,74	0,001	1,41

Regression Equation in Coded Units

MaxTime = 99,28 - 0,1352 P + 0,001592 P*P - 0,0800 W*L

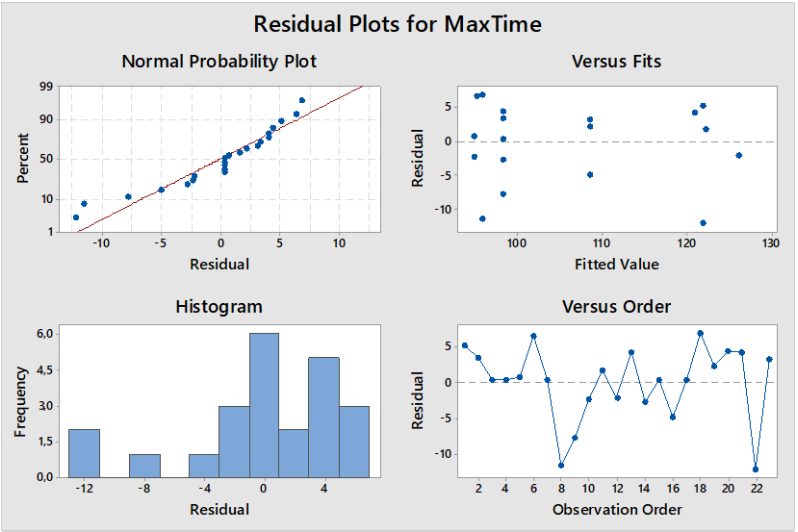

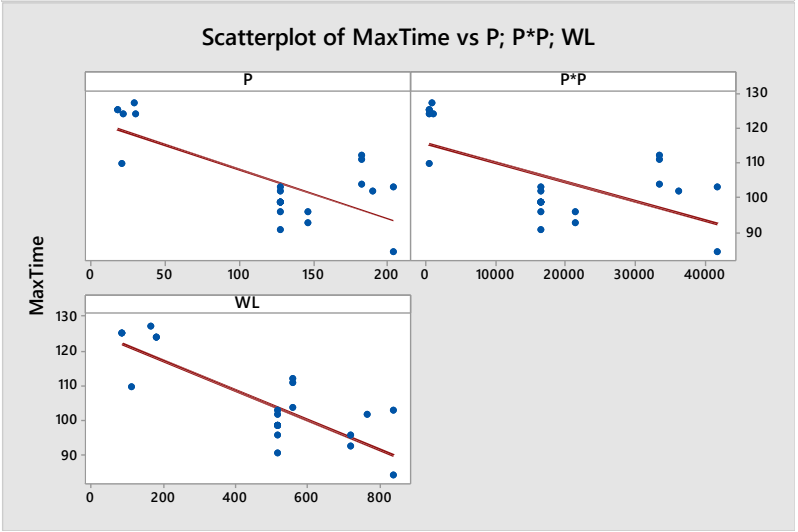

AREA 9:

Number of data: 22

Analysis of Variance

Source	DF	Adj SS	Adj MS	F-Value	P-Value
Regression	3	4225,9	1408,62	32,11	0,000
L	1	2999,0	2998,98	68,37	0,000
B*B	1	209,1	209,13	4,77	0,042
W*L	1	173,2	173,22	3,95	0,062
Error	18	789,6	43,87		
Total	21	5015,5			

Model Summary

S	R-sq	R-sq(adj)	R-sq(pred)
6,62320	84,26%	81,63%	77,18%

Coded Coefficients

Term	Coef	SE Coef	T-Value	P-Value	VIF
Constant	105,81	2,63	40,24	0,000	
L	-0,7494	0,0906	-8,27	0,000	1,55
B*B	0,000027	0,000012	2,18	0,042	1,09
W*L	-0,0718	0,0361	-1,99	0,062	1,56

Regression Equation in Coded Units

MaxTime = 105,81 - 0,7494 L + 0,000027 B*B - 0,0718 W*L

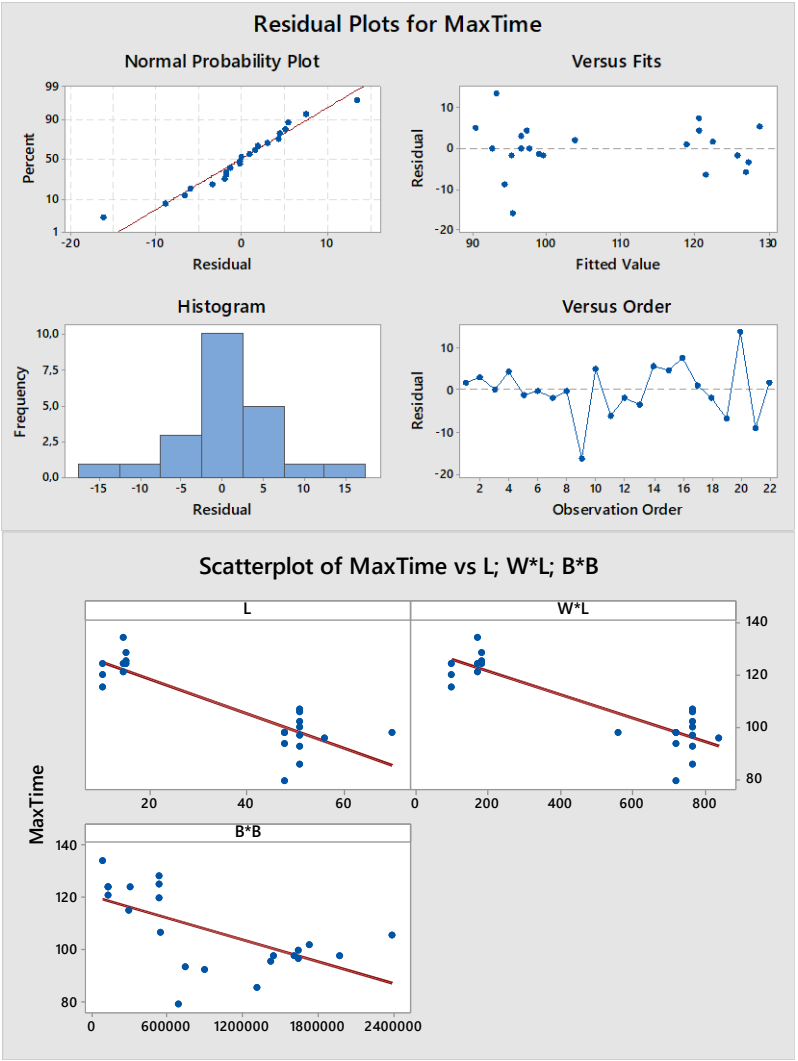

AREA 10:

Number of data: 31

Analysis of Variance

Source	DF	Adj SS	Adj MS	F-Value	P-Value
Regression	4	7407,3	1851,84	43,41	0,000
B	1	162,2	162,21	3,80	0,062
W	1	2516,6	2516,57	58,99	0,000
B*P	1	210,1	210,14	4,93	0,035
B*W	1	122,8	122,83	2,88	0,102
Error	26	1109,2	42,66		
Total	30	8516,5			

Model Summary

S	R-sq	R-sq(adj)	R-sq(pred)
6,53148	86,98%	84,97%	81,13%

Coded Coefficients

Term	Coef	SE Coef	T-Value	P-Value	VIF
Constant	109,19	1,58	69,05	0,000	
B	-0,00861	0,00441	-1,95	0,062	2,52
W	-5,848	0,761	-7,68	0,000	2,15
B*P	0,000216	0,000098	2,22	0,035	3,87
B*W	-0,00651	0,00384	-1,70	0,102	4,64

Regression Equation in Coded Units

MaxTime = 109,19 - 0,00861 B - 5,848 W + 0,000216 B*P - 0,00651 B*W

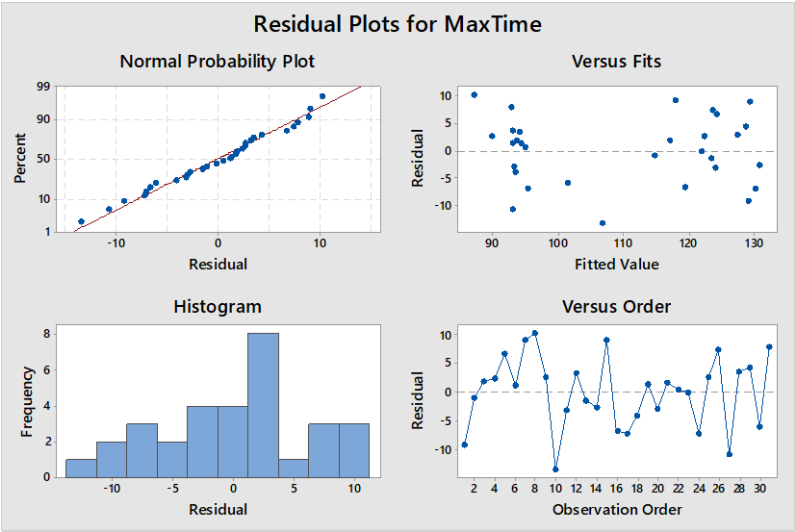

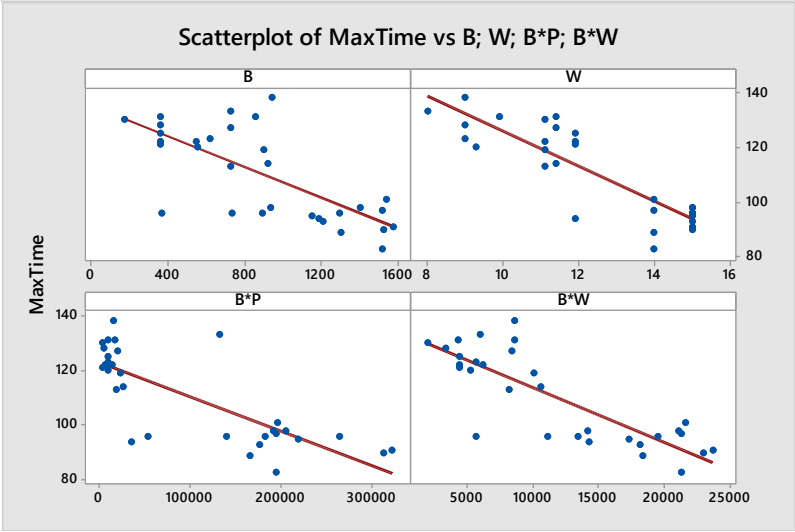

AREA 11:

Number of data: 36

Analysis of Variance

Source	DF	Adj SS	Adj MS	F-Value	P-Value
Regression	2	1438,4	719,19	27,96	0,000
B	1	242,8	242,83	9,44	0,004
W*F	1	1175,8	1175,83	45,72	0,000
Error	33	848,7	25,72		
Total	35	2287,1			

Model Summary

S	R-sq	R-sq(adj)	R-sq(pred)
5,07145	62,89%	60,64%	50,75%

Coded Coefficients

Term	Coef	SE Coef	T-Value	P-Value	VIF
Constant	129,140	0,867	149,01	0,000	
B	0,00711	0,00231	3,07	0,004	1,00
W*F	0,2278	0,0337	6,76	0,000	1,00

Regression Equation in Coded Units

MaxTime = 129,140 + 0,00711 B + 0,2278 W*F

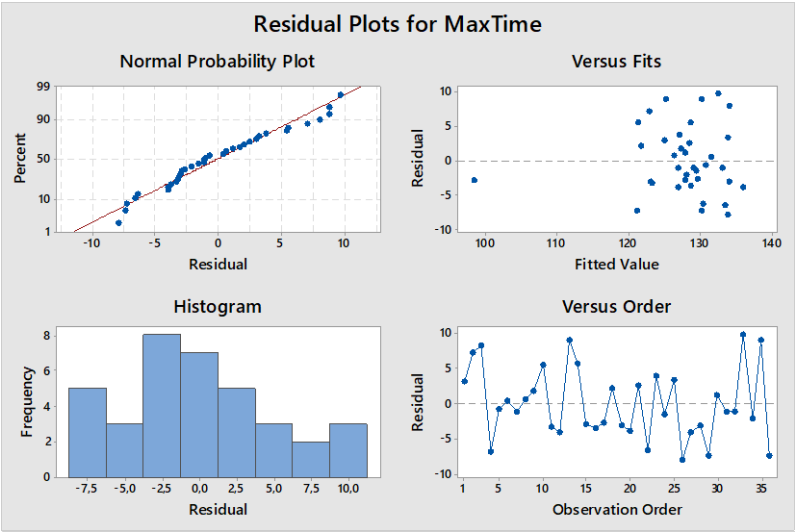

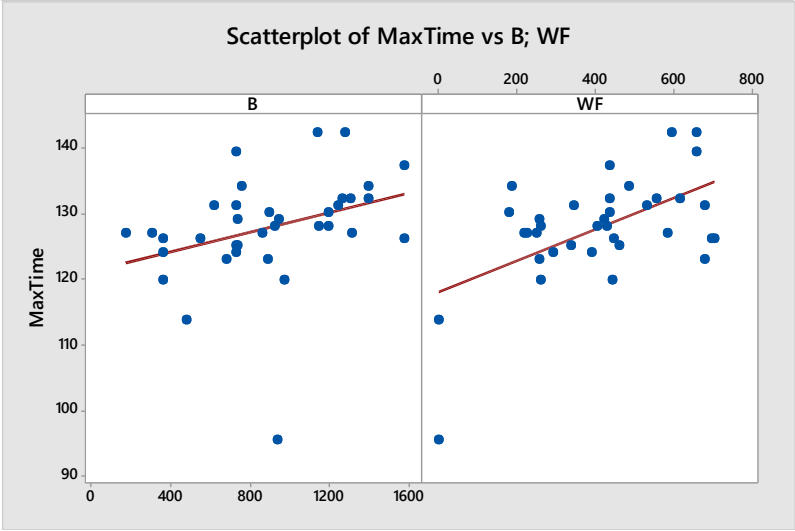

AREA 12:

Number of data: 78

Analysis of Variance

Source	DF	Adj SS	Adj MS	F-Value	P-Value
Regression	3	9673,6	3224,53	58,66	0,000
B	1	931,6	931,62	16,95	0,000
W	1	168,0	168,03	3,06	0,085
L*L	1	4577,9	4577,86	83,28	0,000
Error	74	4067,9	54,97		
Lack-of-Fit	63	3712,8	58,93	1,83	0,137
Pure Error	11	355,0	32,28		
Total	77	13741,5			

Model Summary

S	R-sq	R-sq(adj)	R-sq(pred)
7,41426	70,40%	69,20%	65,64%

Coded Coefficients

Term	Coef	SE Coef	T-Value	P-Value	VIF
Constant	125,868	0,872	144,37	0,000	
B	0,00890	0,00216	4,12	0,000	1,08
W	-1,257	0,719	-1,75	0,085	1,66
L*L	-0,02648	0,00290	-9,13	0,000	1,77

Regression Equation in Coded Units

MaxTime = 125,868 + 0,00890 B - 1,257 W - 0,02648 L*L

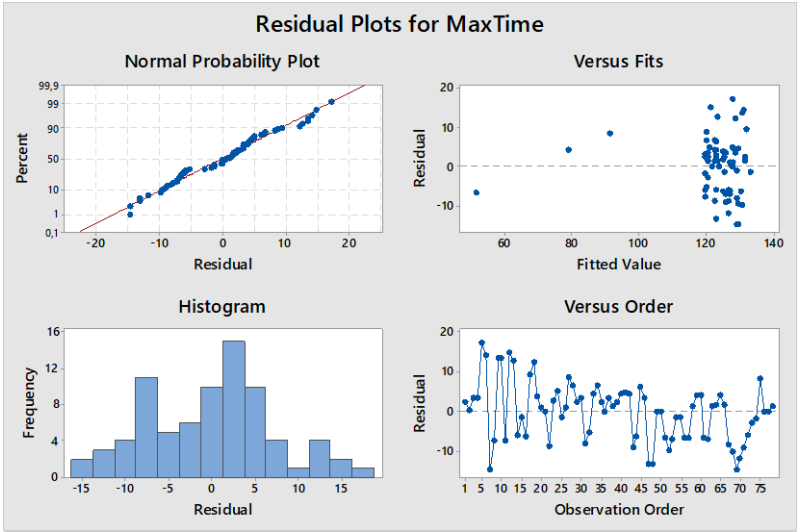

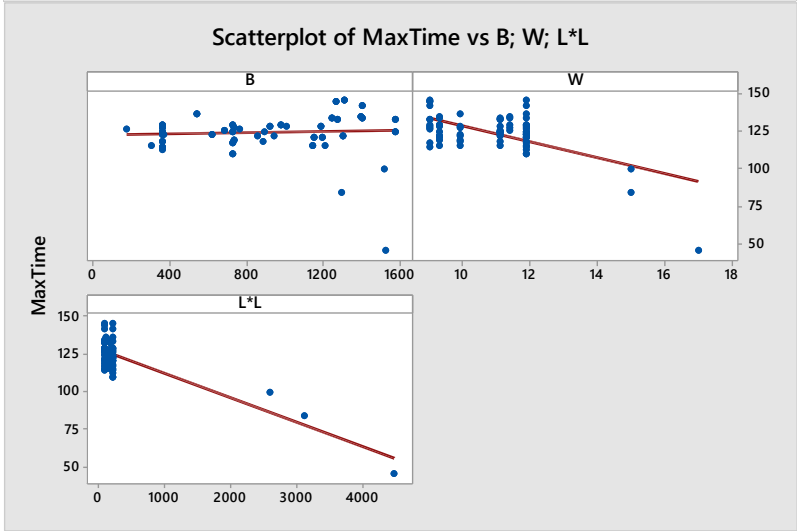

AREA 13:

Number of data: 17

Analysis of Variance

Source	DF	Adj SS	Adj MS	F-Value	P-Value
Regression	2	3575,2	1787,59	81,44	0,000
P	1	527,7	527,67	24,04	0,000
L*L	1	1055,0	1054,97	48,06	0,000
Error	14	307,3	21,95		
Total	16	3882,5			

Model Summary

S	R-sq	R-sq(adj)	R-sq(pred)
4,68512	92,08%	90,95%	88,38%

Coded Coefficients

Term	Coef	SE Coef	T-Value	P-Value	VIF
Constant	92,89	1,87	49,57	0,000	
P	-0,0995	0,0203	-4,90	0,000	1,47
L*L	0,02839	0,00410	6,93	0,000	1,47

Regression Equation in Coded Units

MaxTime = 92,89 - 0,0995 P + 0,02839 L*L

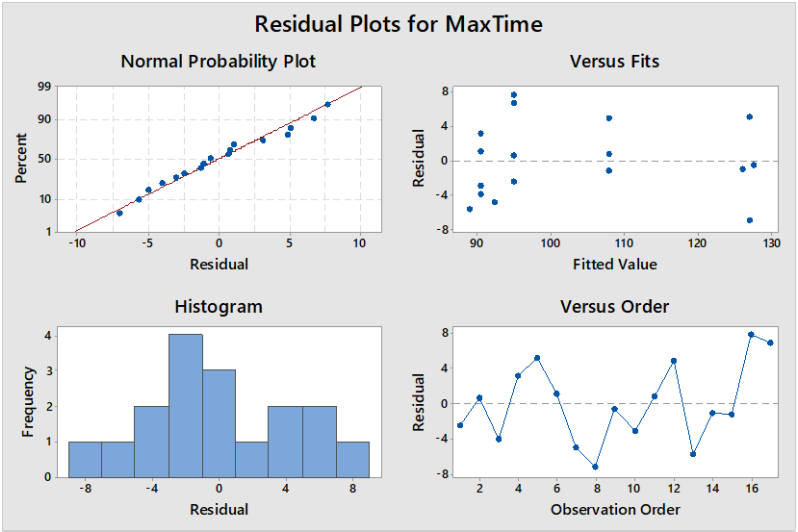

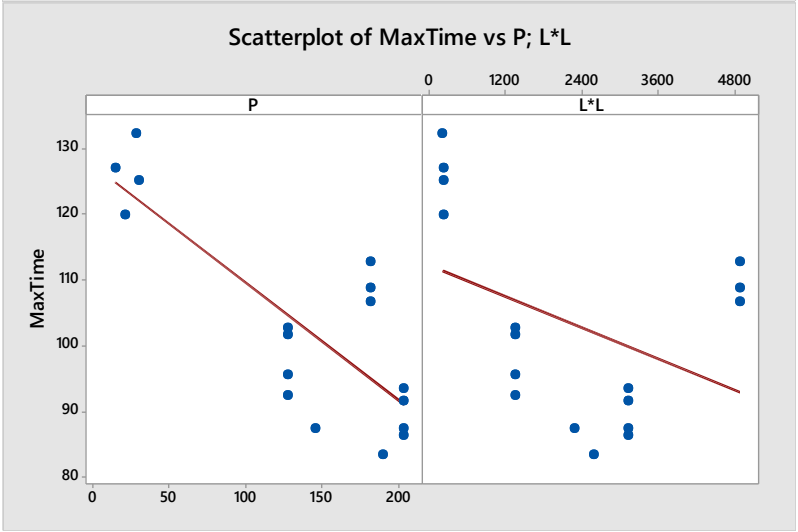

AREA 14:

Number of data: 30

Analysis of Variance

Source	DF	Adj SS	Adj MS	F-Value	P-Value
Regression	5	6001,98	1200,40	56,86	0,000
B	1	227,88	227,88	10,79	0,003
L	1	1401,31	1401,31	66,38	0,000
W	1	186,54	186,54	8,84	0,007
L*L	1	974,41	974,41	46,16	0,000
B*W	1	81,69	81,69	3,87	0,061
Error	24	506,64	21,11		
Total	29	6508,61			

Model Summary

S	R-sq	R-sq(adj)	R-sq(pred)
4,59455	92,22%	90,59%	88,26%

Coded Coefficients

Term	Coef	SE Coef	T-Value	P-Value	VIF
Constant	97,13	1,72	56,37	0,000	
B	0,01139	0,00347	3,29	0,003	2,23
L	-0,4819	0,0592	-8,15	0,000	2,02
W	-1,324	0,445	-2,97	0,007	2,13
L*L	0,02564	0,00377	6,79	0,000	2,66
B*W	-0,00253	0,00129	-1,97	0,061	1,46

Regression Equation in Uncoded Units

MaxTime = 136,1 + 0,0444 B - 2,645 L + 1,20 W + 0,02564 L*L - 0,00253 B*W

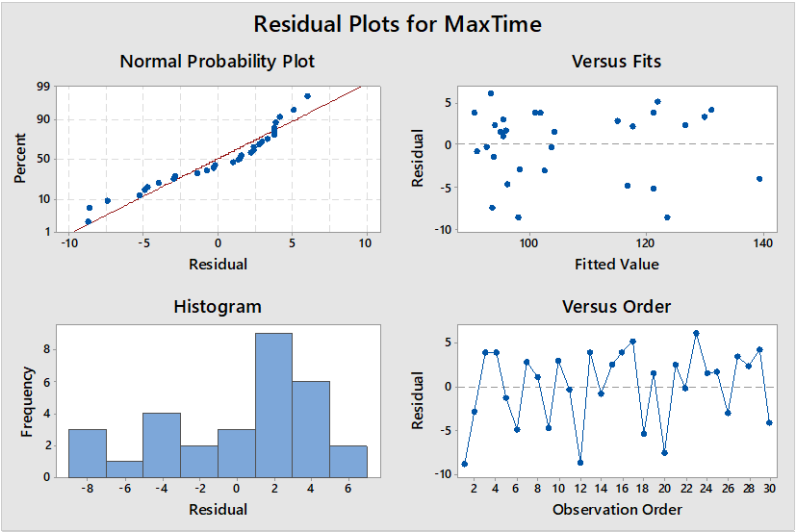

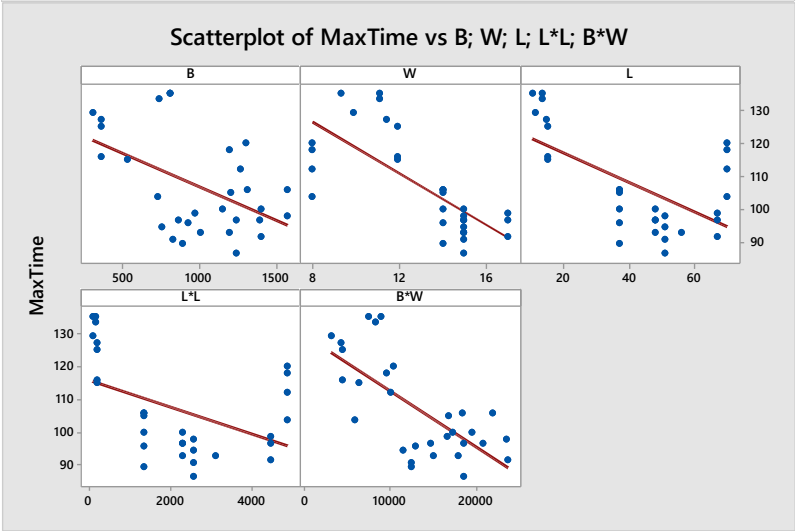

AREA 15:

Number of data: 32

Analysis of Variance

Source	DF	Adj SS	Adj MS	F-Value	P-Value
Regression	5	4376,02	875,20	40,02	0,000
P	1	906,09	906,09	41,43	0,000
W	1	75,58	75,58	3,46	0,074
P*P	1	435,50	435,50	19,91	0,000
B*F	1	108,17	108,17	4,95	0,035
L*W	1	212,30	212,30	9,71	0,004
Error	26	568,65	21,87		
Total	31	4944,67			

Model Summary

S	R-sq	R-sq(adj)	R-sq(pred)
4,67666	88,50%	86,29%	83,53%

Coded Coefficients

Term	Coef	SE Coef	T-Value	P-Value	VIF
Constant	104,69	2,28	45,91	0,000	
P	-0,1512	0,0235	-6,44	0,000	4,84
W	-1,110	0,597	-1,86	0,074	3,52
P*P	0,001738	0,000390	4,46	0,000	2,79
B*F	0,000082	0,000037	2,22	0,035	1,16
L*W	-0,0614	0,0197	-3,12	0,004	2,07

Regression Equation in Coded Units

MaxTime = 104,69 - 0,1512 P - 1,110 W + 0,001738 P*P
+ 0,000082 B*F - 0,0614 L*W

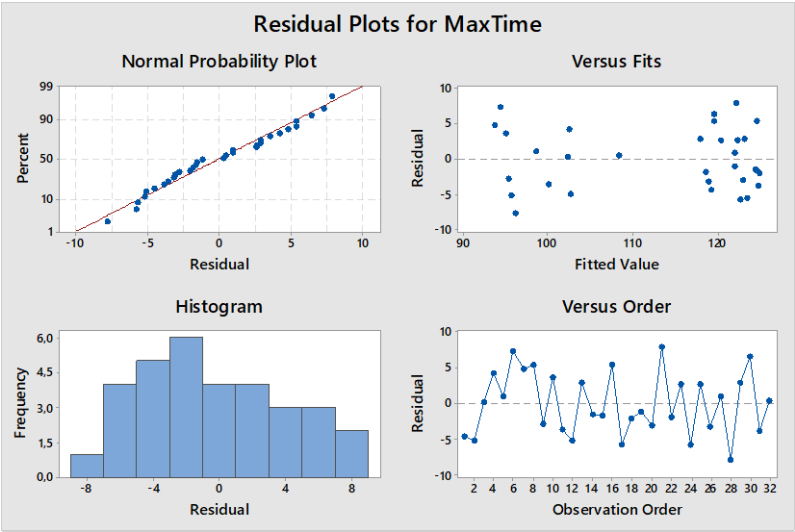

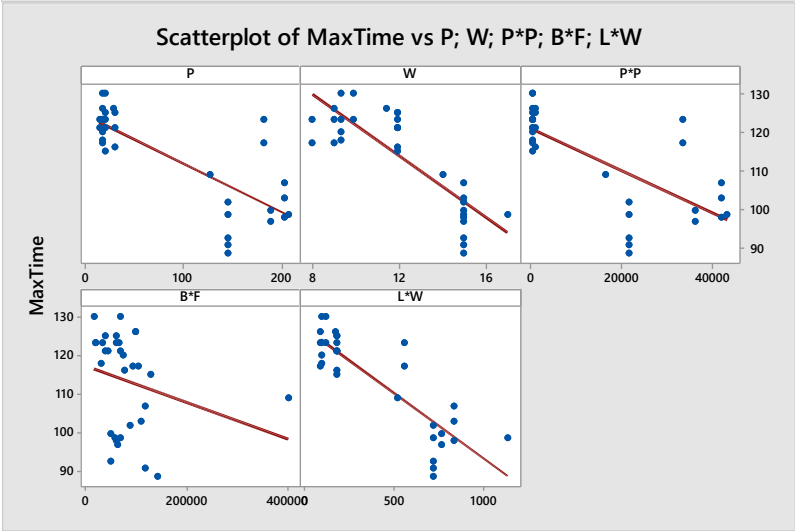

AREA 16:

Number of data: 36

Analysis of Variance

Source	DF	Adj SS	Adj MS	F-Value	P-Value
Regression	4	7893,01	1973,25	56,94	0,000
P	1	2798,41	2798,41	80,75	0,000
B*B	1	137,69	137,69	3,97	0,055
P*P	1	200,78	200,78	5,79	0,022
F*P	1	99,03	99,03	2,86	0,101
Error	31	1074,28	34,65		
Total	35	8967,29			

Model Summary

S	R-sq	R-sq(adj)	R-sq(pred)
5,88678	88,02%	86,47%	85,89%

Coded Coefficients

Term	Coef	SE Coef	T-Value	P-Value	VIF
Constant	114,94	2,63	43,67	0,000	
P	-0,2592	0,0288	-8,99	0,000	3,95
B*B	-0,000019	0,000010	-1,99	0,055	1,59
P *P	0,000971	0,000403	2,41	0,022	3,65
F*P	0,000275	0,000162	1,69	0,101	1,29

Regression Equation in Coded Units

MaxTime = 114,94 - 0,2592 P - 0,000019 B*B + 0,000971 P*P + 0,000275 F*P

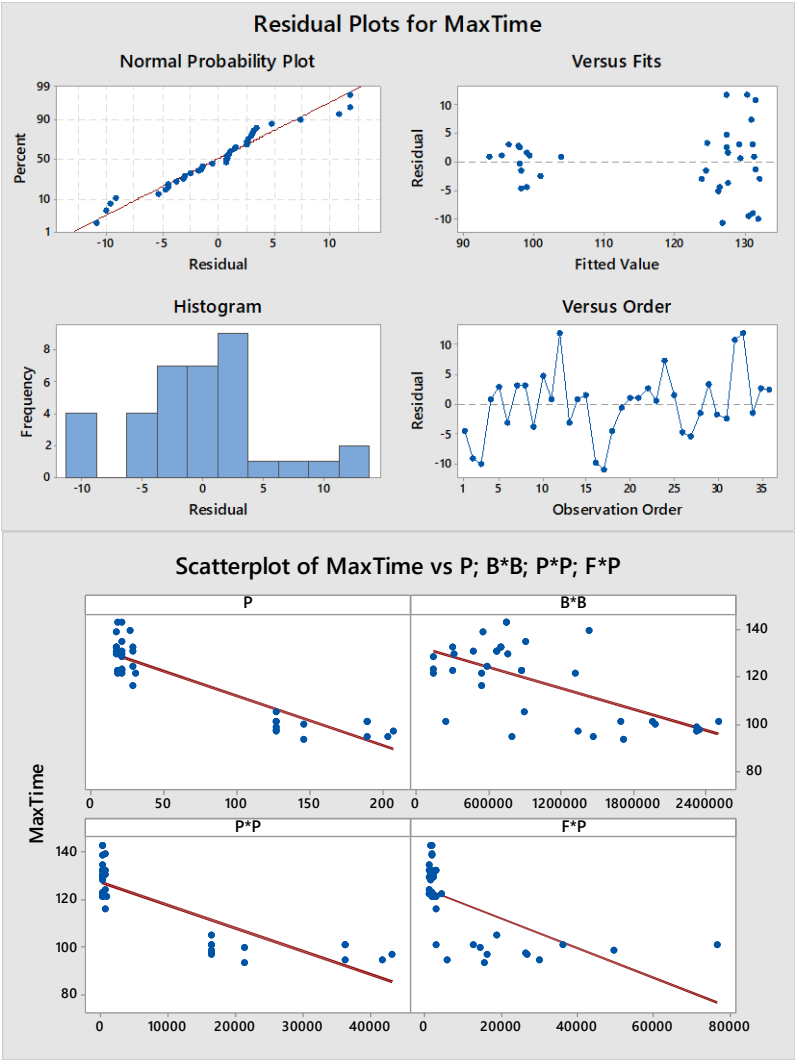

AREA 17:

Number of data: 43

Analysis of Variance

Source	DF	Adj SS	Adj MS	F-Value	P-Value
Regression	1	1728	1727,93	61,87	0,000
P	1	1728	1727,93	61,87	0,000
Error	41	1145	27,93		
Total	42	2873			

Model Summary

S	R-sq	R-sq(adj)	R-sq(pred)
5,28465	60,14%	59,17%	56,29%

Coded Coefficients

Term	Coef	SE Coef	T-Value	P-Value	VIF
Constant	123,443	0,806	153,17	0,000	
P	-0,2080	0,0264	-7,87	0,000	1,00

Regression Equation in Uncoded Units

MaxTime = 129,61 - 0,2080 P

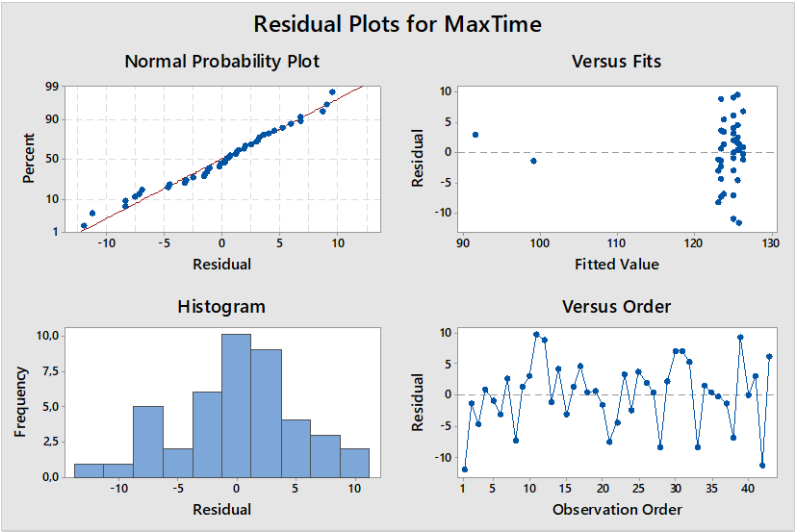

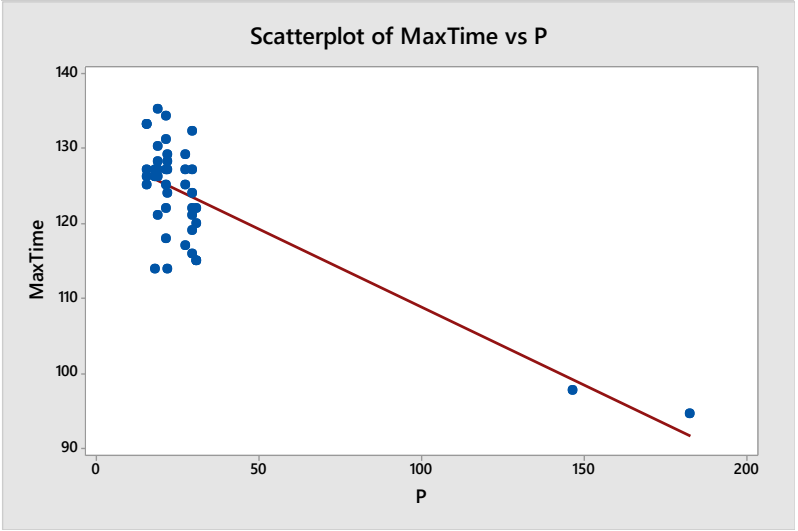

AREA 18:

Number of data: 50

Analysis of Variance

Source	DF	Adj SS	Adj MS	F-Value	P-Value
Regression	1	2240	2240,06	40,94	0,000
P	1	2240	2240,06	40,94	0,000
Error	48	2626	54,72		
Total	49	4866			

Model Summary

S	R-sq	R-sq(adj)	R-sq(pred)
7,39710	46,03%	44,91%	38,55%

Coded Coefficients

Term	Coef	SE Coef	T-Value	P-Value	VIF
Constant	123,26	1,05	117,83	0,000	
P	-0,1368	0,0214	-6,40	0,000	1,00

Regression Equation in Uncoded Units

MaxTime = 128,30 - 0,1368 P

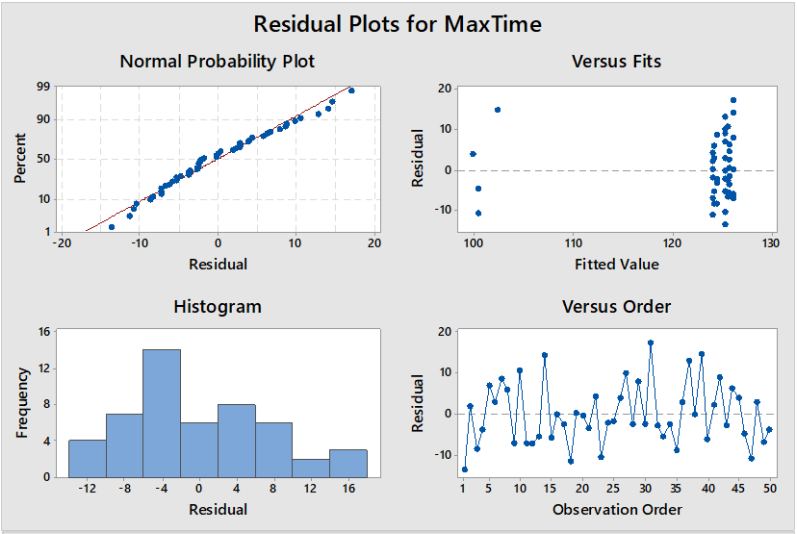

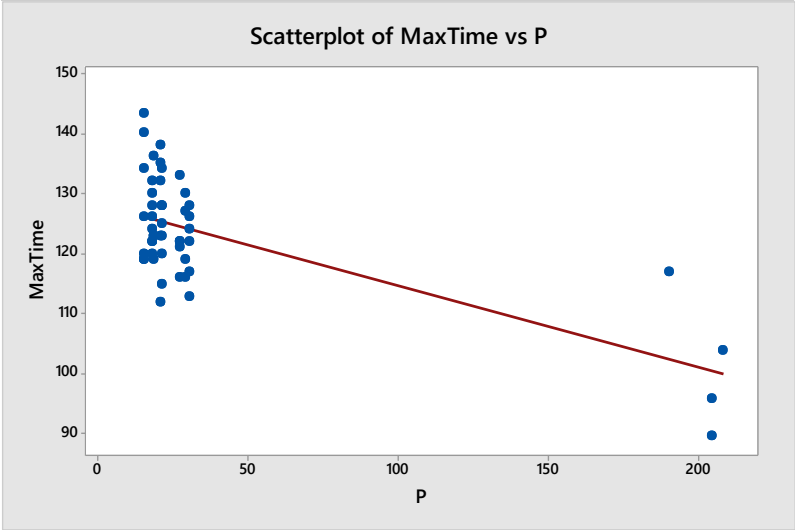

APPENDIX B

Mixed Integer Linear Programming Formulation (Model L)

Sets and Indices

$i \in I = \{1,\ldots,18\}$	Set of composite parts
$j,k \in J = \{1,\ldots,18\}$	Set of areas in autoclave charge floor
$a \in A = \{1,2,3\}$	Set of vertical divisions in the autoclave
$l \in L = \{1,\ldots,13\}$	Set of predictor variables without the term F
$u \in U = \{1,\ldots,4\}$	Set of predictor variables including the term F

Parameters

P_i	Weight of part i
L_i	Length of part i
W_i	Width of part i
H	Maximum number of parts that can be placed horizontally in the autoclave
W	Width of the autoclave
L	Length of the autoclave
β_{jl}	Regression coefficient of predictor variable $l \in L$ in area j
β_{ju}	Regression coefficient of predictor variable $u \in U$ in area j
c_{il}	The value of predictor variable $l \in L$ of part i
d_{iu}	The partial value of predictor variable $u \in U$ of part i that is made of the terms not including F; d_{i1}=1, d_{i2}= B, d_{i3}=P_i, d_{i4}= W_i for all $i \in I$
$\bar{c}_{jl}$	Average of the observed values of predictor variable $l \in L$ in area j
$\bar{d}_{ju}$	Average of the observed values of predictor variable $u \in U$ in area j that is made of the terms not including F
$\bar{f}_j$	Average of the observed values of front part weights in area j

Decision Variables

x_{ij}	= 1, if part i is placed in area j; 0, otherwise
f_j	Total part weight in front of area j
y_j	The maximum length of the parts placed in area j
t_{lead}	Time to reach the curing temperature for the leading part
t_{lag}	Time to reach the curing temperature for the lagging part
t_i	Time to reach the curing temperature for part i

$$\min z_1 = t_{lag} - t_{lead} \tag{1}$$

$$\min z_2 = t_{lag} \tag{2}$$

Subject to

$$t_i = \sum_{j=1}^{18} x_{ij} \sum_{l=1}^{13} \beta_{jl} \left(c_{il} - \bar{c}_{jl}\right) + \sum_{j=1}^{18} \sum_{u=1}^{4} e_{iju} \qquad \forall\, i \in I \tag{3*}$$

$$\sum_{j=1}^{18} x_{ij} = 1 \qquad \forall\, i \in I \tag{4}$$

$$\sum_{i=1}^{18} x_{ij} \leq 2 \qquad \forall\, j \in J \tag{5}$$

$$\sum_{i=1}^{18} (x_{i,j} + x_{i,j+6} + x_{i,j+12}) \leq H \qquad j = 1, \dots, 6 \tag{6}$$

$$\sum_{i=1}^{18} W_i (x_{i,j} + x_{i,j+6} + x_{i,j+12}) \leq W \qquad j = 1, \dots, 6 \tag{7}$$

$$y_j + y_{j+1} + y_{j+2} + y_{j+3} + y_{j+4} + y_{j+5} \leq L \qquad j = 1,7,13 \tag{8}$$

$$y_j \geq L_i x_{ij} \qquad \forall\, i \in I, j \in J \tag{9}$$

$$f_j = \sum_{k=j+1}^{6a} \sum_{i=1}^{18} P_i x_{ik} \qquad a \in A,\ j = 6a - 5, \dots, 6a - 1 \tag{10}$$

$$t_{lag} \geq t_i \qquad \forall\, i \in I \tag{11}$$

$$t_{lead} \leq t_i \qquad \forall\, i \in I \tag{12}$$

$$x_{ij} \in \{0,1\} \qquad \forall\, i \in I, j \in J \tag{13}$$

$$e_{iju} \leq M x_{ij} \qquad \forall\, i \in I, j \in J, u \in U \tag{14}$$

$$e_{iju} \geq -M x_{ij} \qquad \forall\, i \in I, j \in J, u \in U \tag{15}$$

$$e_{iju} \leq \beta_{ju} \left(d_{iu} - \bar{d}_{ju}\right)\left(f_j - \bar{f}_j\right) + M(1 - x_{ij}) \qquad \forall\, i \in I, j \in J, u \in U \tag{16}$$

$$e_{iju} \geq \beta_{ju} (d_{iu} - \bar{d}_{ju})(f_j - \bar{f}_j) - M(1 - x_{ij}) \qquad \forall\, i \in I, j \in J, u \in U \tag{17}$$